Extinction Distances to and Dust Properties of the Supernova Remnants

Biwei Jiang 姜碧沩 bjiang@bnu.edu.cn
Department of Astronomy, Beijing Normal University
Key Collaborators: He Zhao（赵赫） Shu Wang（王舒）Jun Li（李军）

Distances to Supernova Remnants

- Essential to investigate the properties of SNR
- Pervious methods
  - The HI or CO line velocity in combination with the Galactic rotation curve
    - Uncertainty: Non-circular motion, ambiguity
    - Ilovaisky & Lequeux (1972) , Leahy & Tian (2008a,b, 2010) and Tian & Leahy (2013)
  - The empirical power-law relation between the radio brightness and the linear diameter ($\Sigma_\nu(D) = AD^{-\beta}$)
    - Uncertainty: the power-law index varies from about 2 to 6
    - Case & Bhattacharya 1998; Guseinov et al. 2003; Pavlovic et al. 2013
    - Dispersion: the index error can be as large as 40% (Zhu & Tian 2014)
  - Other non-popular methods
    - The distance of the associated source (Green 1984)
    - Proper motion, in combination with expansion velocity (Green 1984).
    - The X-ray flux (Kassim et al. 1994): the X-ray temperature is an indictor of the shock velocity in the Sedov phase

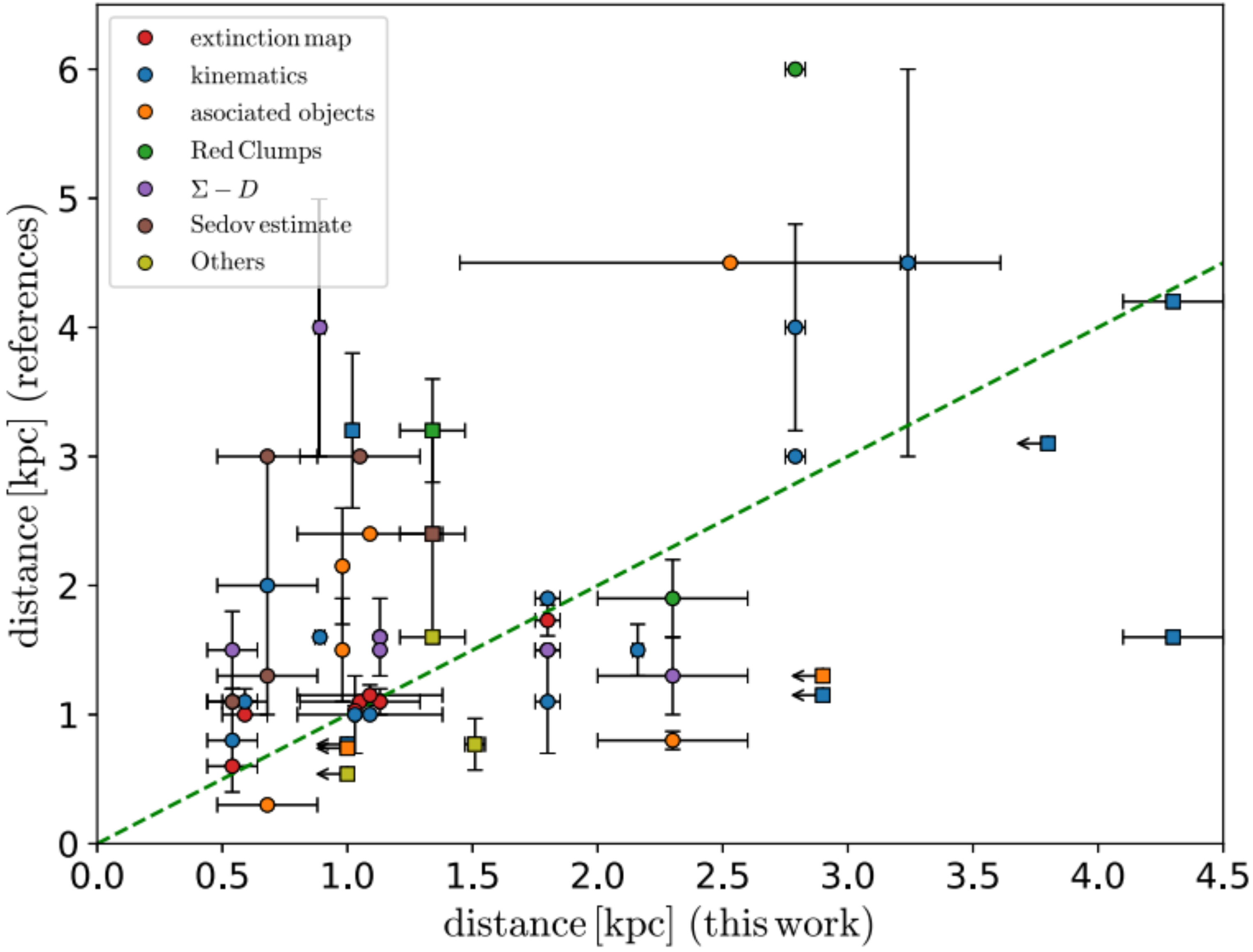

Figure 8. The comparison between our results and the distances measured by other methods for SNRs in Level A and B. Dots and squares decode SNRs in Level A and B, respectively. Squares with left arrows are the cases with

Zhao+2020

The extinction-distance model

At the position of a SNR, the extinction increases sharply due to its (and the associated molecular cloud's) higher dust density than fore- and back-ground ISM

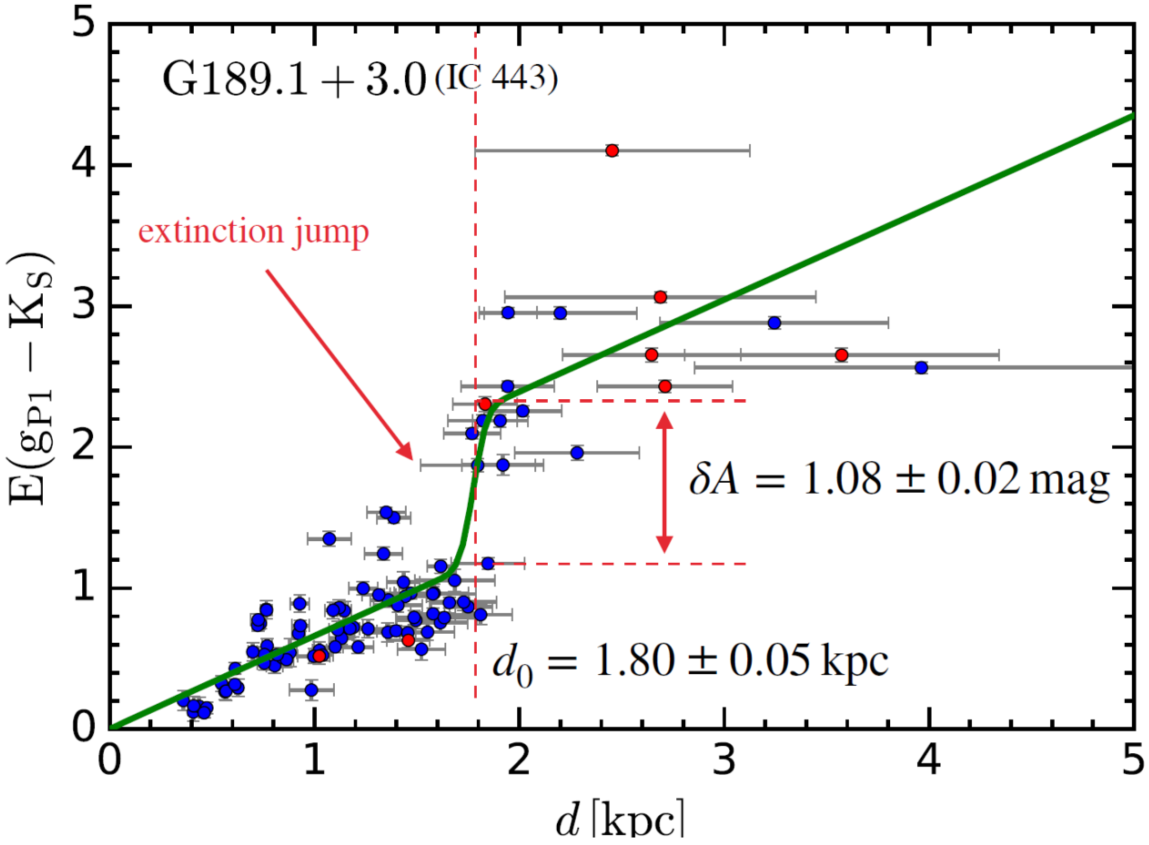

$$A(d) = A^0(d) + A^1(d)$$

$$A^0(d) = a \times d + b \times \sqrt{d}$$

$$A^1(d) = \frac{\delta A}{2} \times \left[1 + erf\left(\frac{d - d_0}{\sqrt{2}\,\delta d}\right)\right]$$

Zhao+2020

Key parameter- Distance

- Gaia parallax
  - Large number: 1.46 billion sources (Gaia collaboration 2022)
  - Optical band: relatively shallow, with a limiting magnitude of about G~21 i.e. ~2kpc for a solar-like MS star with A_G=5mag
- Red clump stars ← standard candle: constant M_K ~ −1.6±0.03 (Alves 2000), $C_{JKs}^{0}\sim 0.65\pm 0.02$ (Wang+2020)
  - Bright in near-infrared: detectable at large distance, i.e. 10kpc with A_K=0.5mag for m_K=14mag (JWST ~ 28mag)
  - $5\log(\frac{d}{\mathrm{pc}}) = m_{K_s} - (-1.6) - 0.47\times(C_{JKs} - 0.65) + 5$
    - Assumptions: extinction law, intrinsic color index
    - The distance and extinction are determined for the RC ridge
  - Difficult to separate from other red stars based only on photometry

Selection of red clump stars

1. the branch in the J-Ks/Ks diagram from 2MASS, UKIDSS for the north and VVV for the south

2. exclusion of stars with obvious difference between the RC and Gaia distance

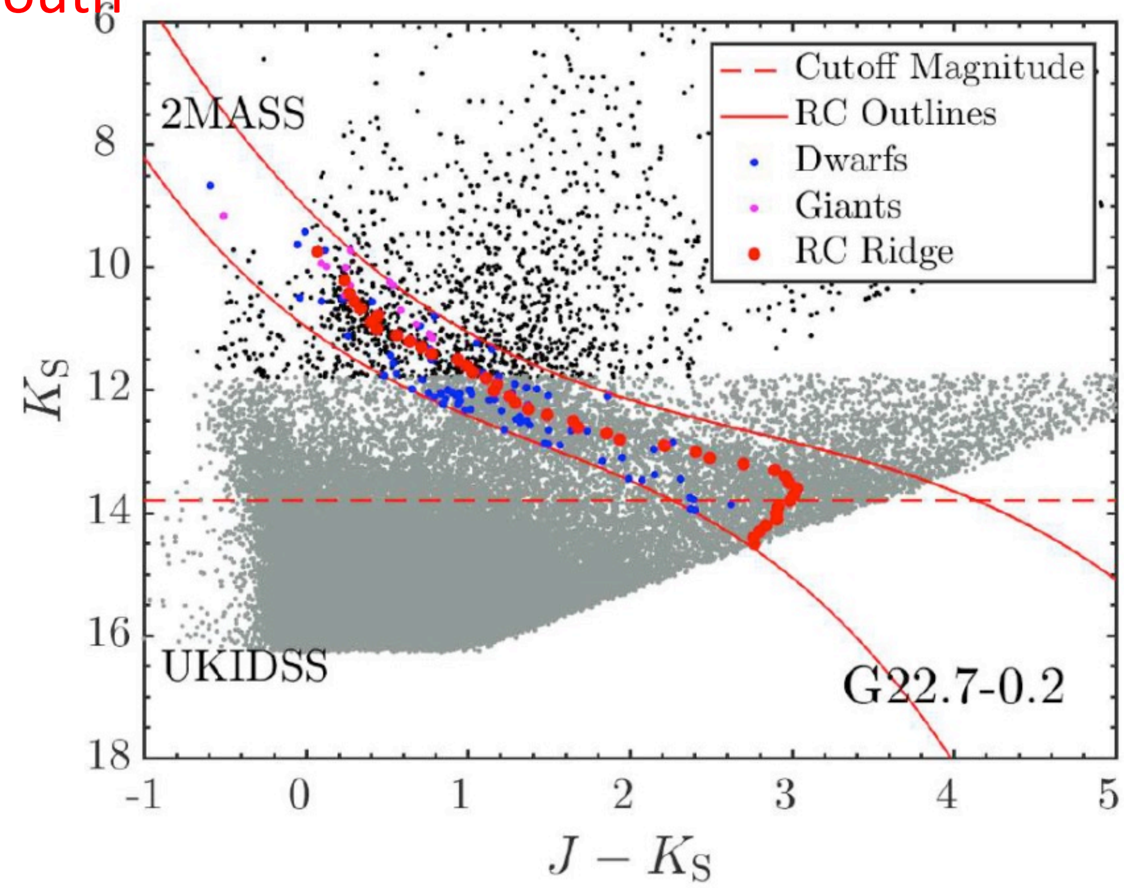

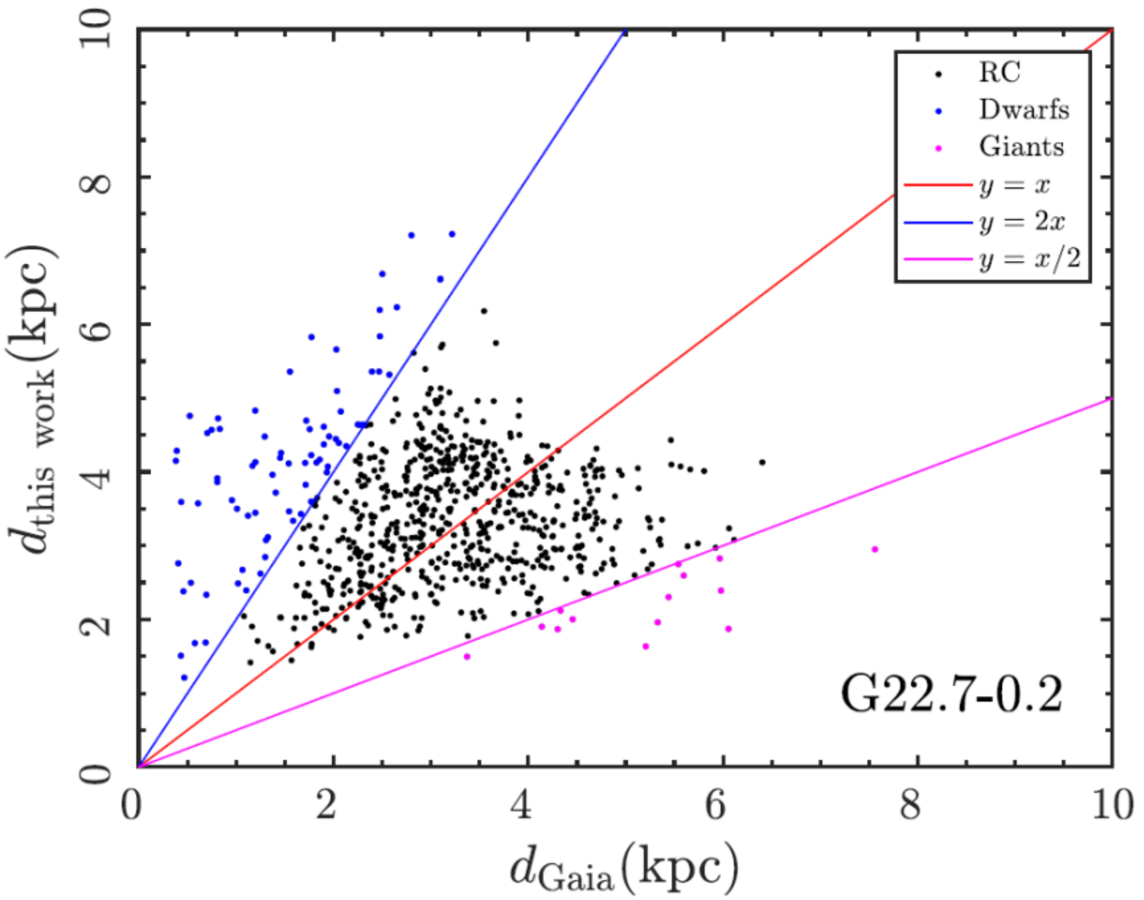

Key parameter – Extinction/Intrinsic color index

- Red clump stars
  - Almost constant $C_{JK}^{0} \cong 0.65 \pm 0.02$ (Wang+2020)
- Blue-edge
  - Stars with no extinction are the bluest among the stars with the same $T_{\rm eff}$, log g and Z (Wang & Jiang 2014)
  - From stellar parameters determined by the spectroscopic surveys – LAMOST for dwarf stars and APOGEE for giant stars

Intrinsic color index: the blue-edge method

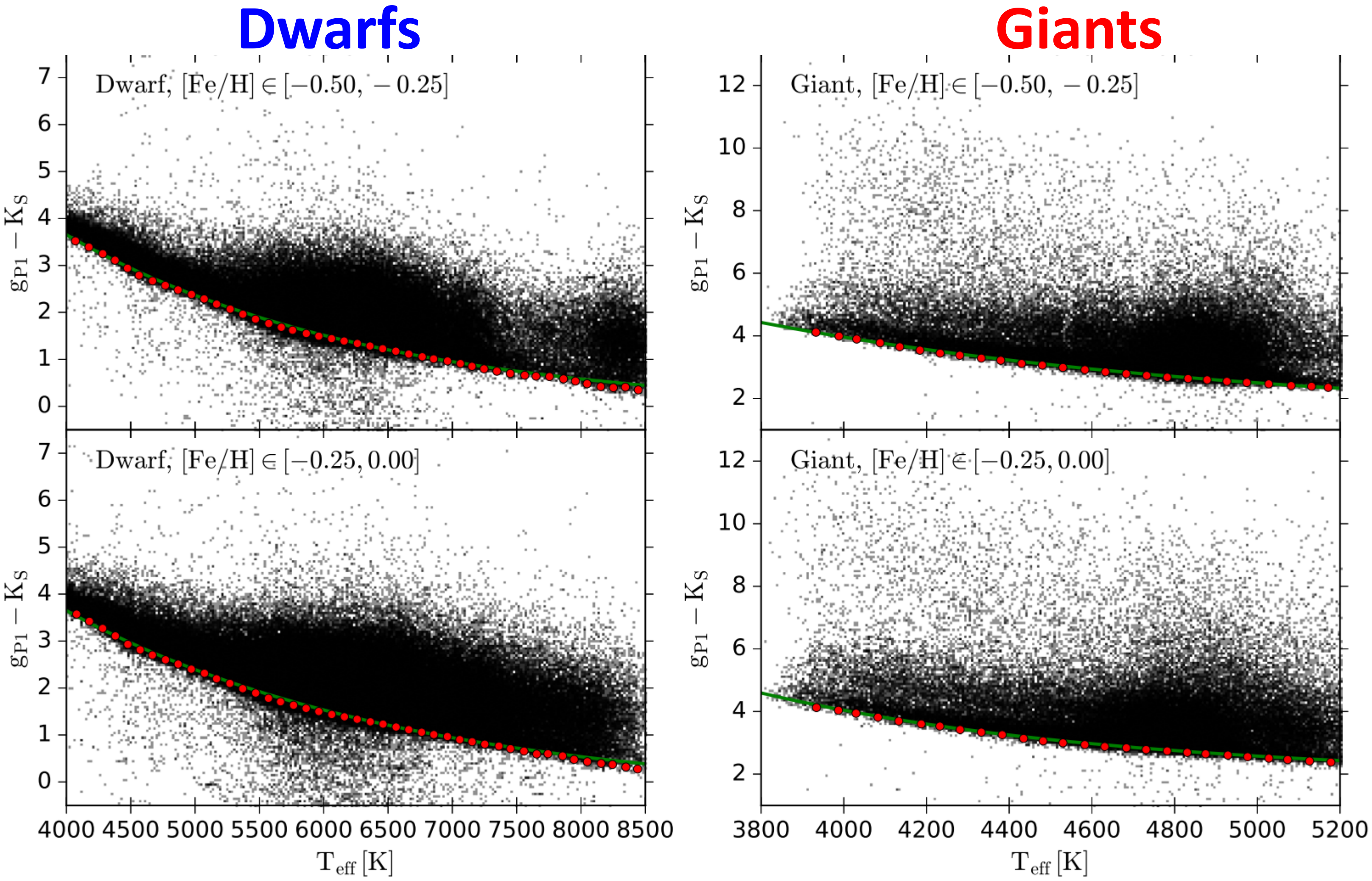

LAMOST: optical low-resolution spectrum of >10^7 stars with *V*mag< 18 mag

APOGEE: H-band high-resolution spectrum for 6×10^5 stars with *H*mag<12.5mag

Pan-STARRS1: optical photometry

Zhao+2018, 2020

The Rosetta Nebula (SNR Mon) at ten color excesses

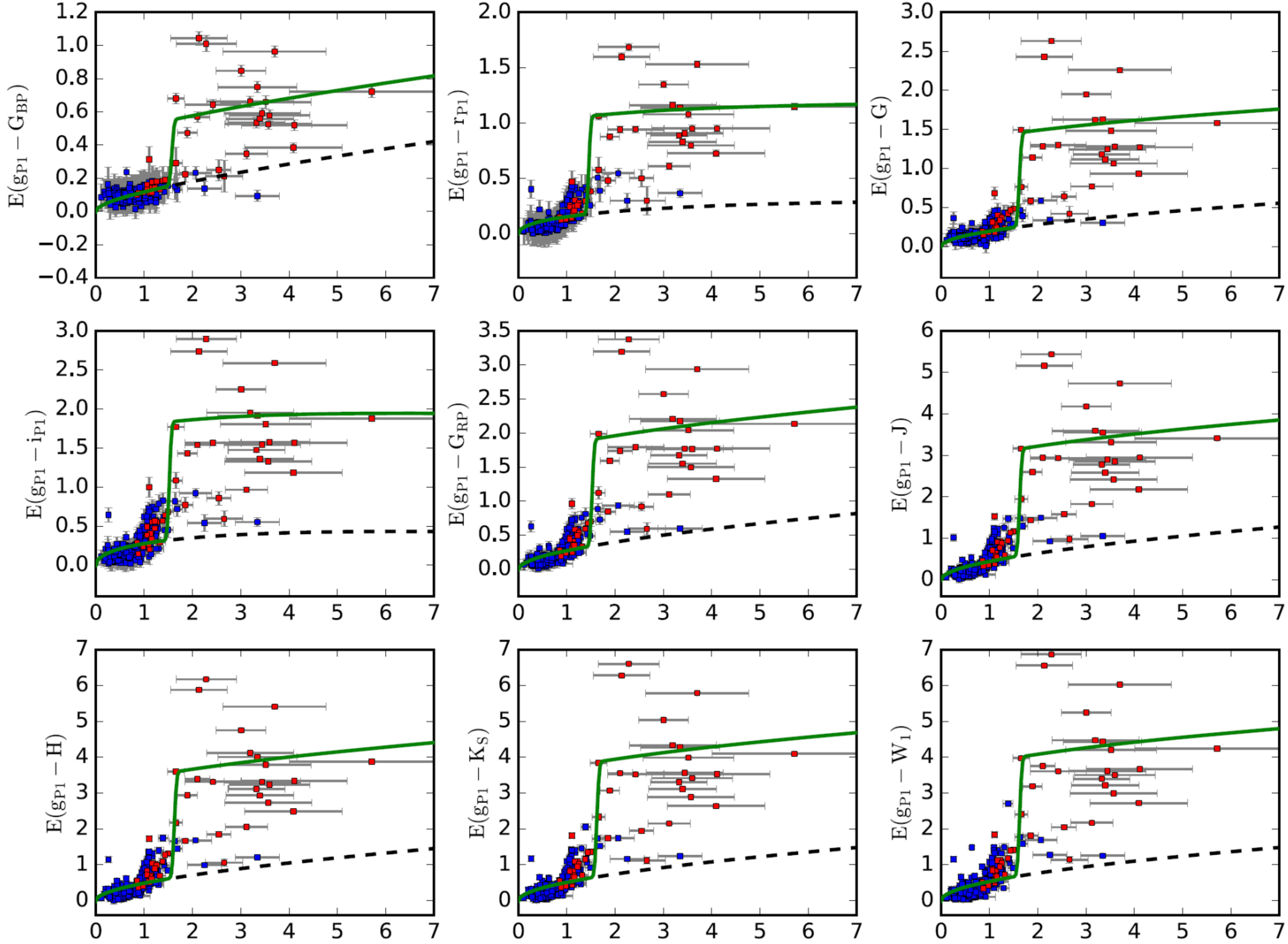

Gaia/G_{BP} G G_{RP}

APASS/gri

Pan-STARRS1/gri

2MASS *JHK*$_S$

WISE/W1,W2

Distance: the average of the fitted distances from the reddenings in five IR bands relative to g_{P1}

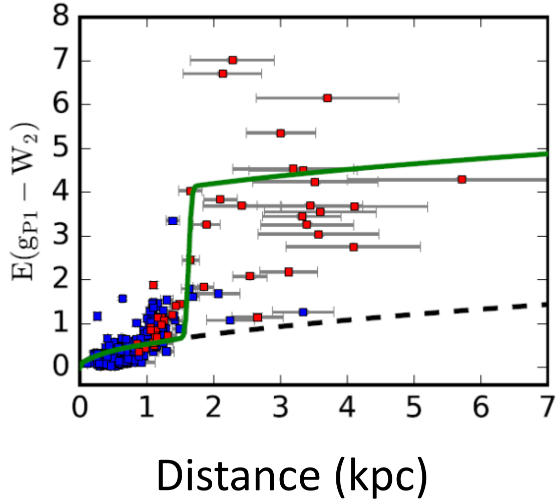

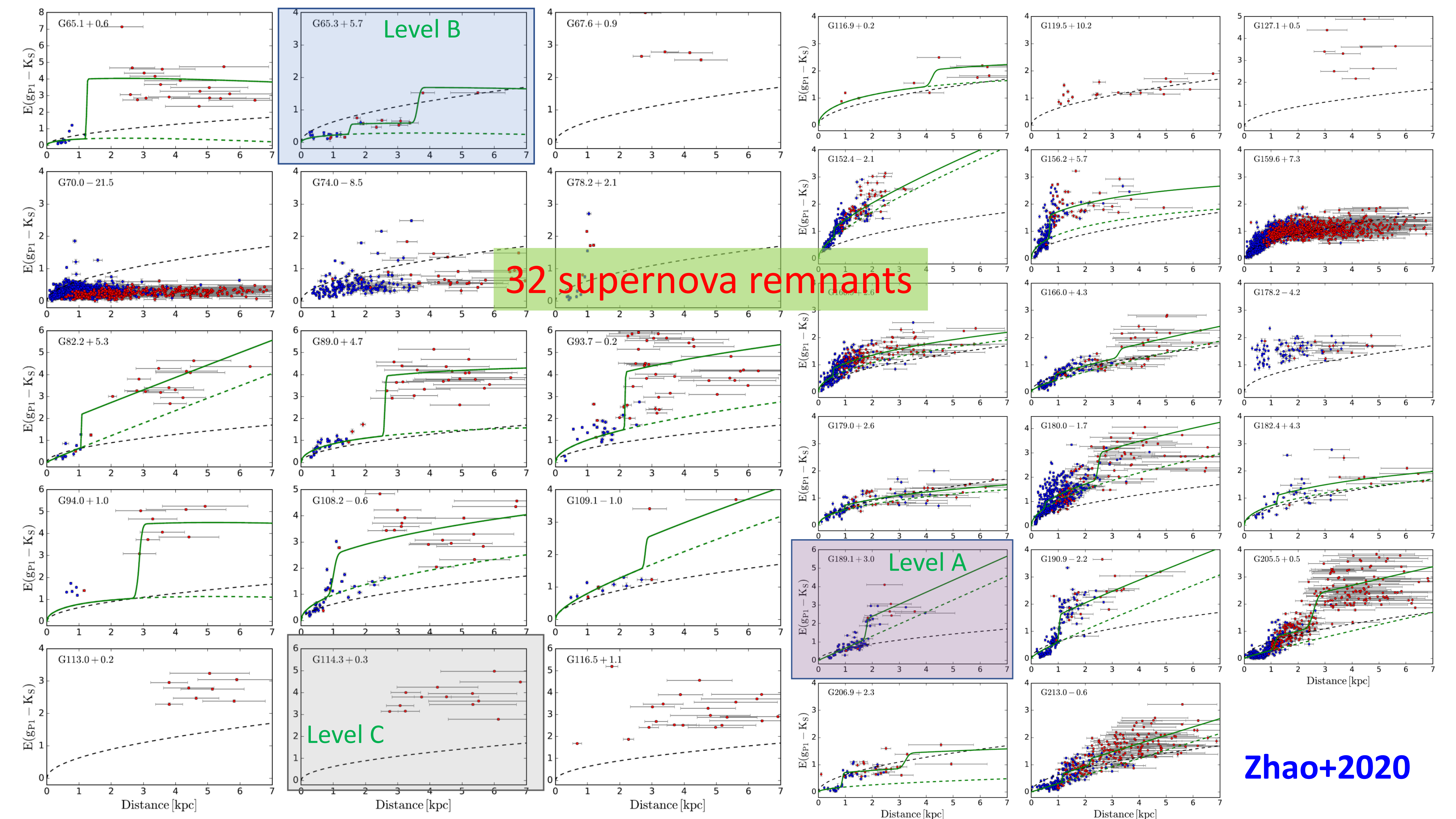

32 supernova remnants
Level A
Level B
Level C
Zhao+2020
G65.1 + 0.6
G65.3 + 5.7
G67.6 + 0.9
G70.0 − 21.5
G74.0 − 8.5
G78.2 + 2.1
G82.2 + 5.3
G89.0 + 4.7
G93.7 − 0.2
G94.0 + 1.0
G108.2 − 0.6
G109.1 − 1.0
G113.0 + 0.2
G114.3 + 0.3
G116.5 + 1.1
G116.9 + 0.2
G119.5 + 10.2
G127.1 + 0.5
G152.4 − 2.1
G156.2 + 5.7
G159.6 + 7.3
G166.0 + 4.3
G178.2 − 4.2
G179.0 + 2.6
G180.0 − 1.7
G182.4 + 4.3
G189.1 + 3.0
G190.9 − 2.2
G205.5 + 0.5
G206.9 + 2.3
G213.0 − 0.6
$E(g_{P1} - K_S)$
Distance [kpc]

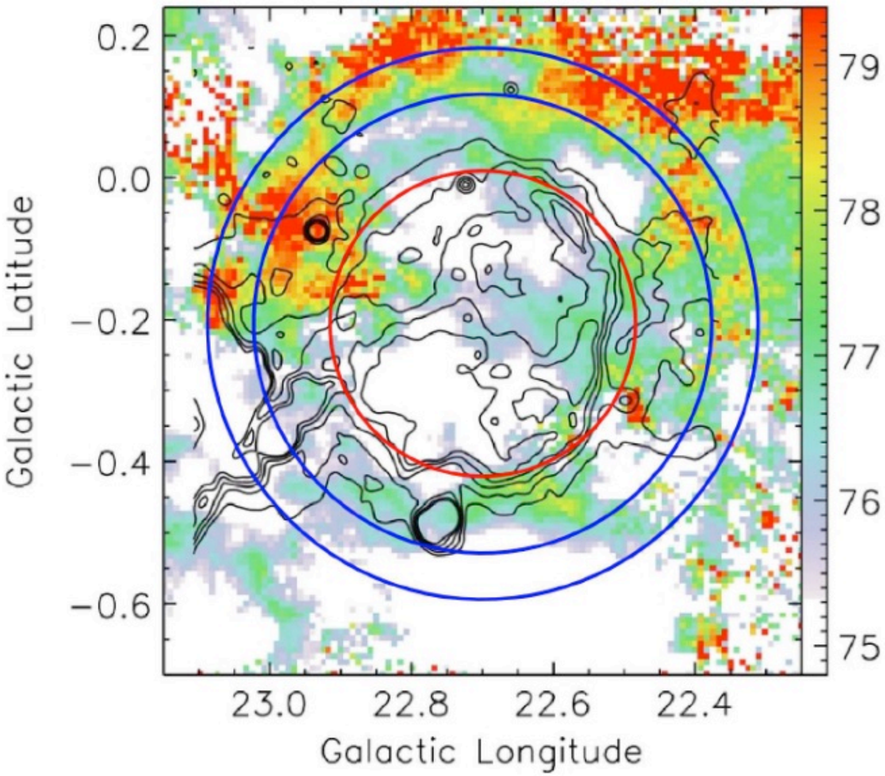

Fig. 3. Definition of the SNR area (the red circle) and the surrounding area (the blue annulus) for SNR G22.7-0.2 as an example. The background image is the ^{13}CO ($J = 1$–0) emission map overlaid with the 1.4 GHz radio continuum emission contours from Su et al. (2014).

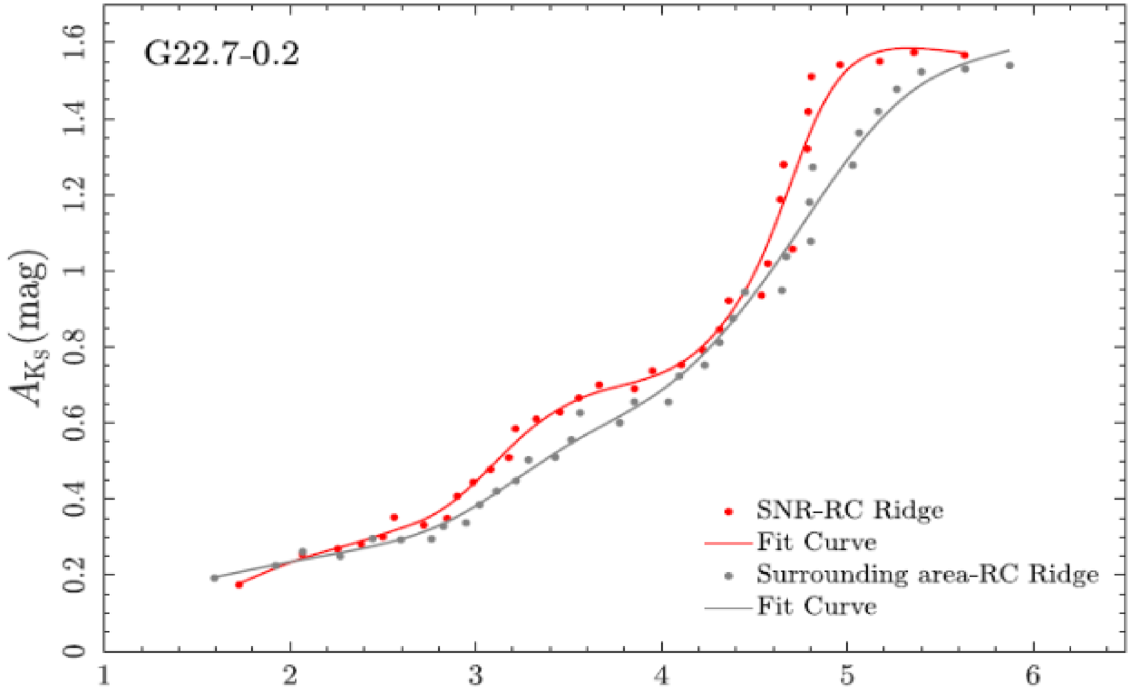

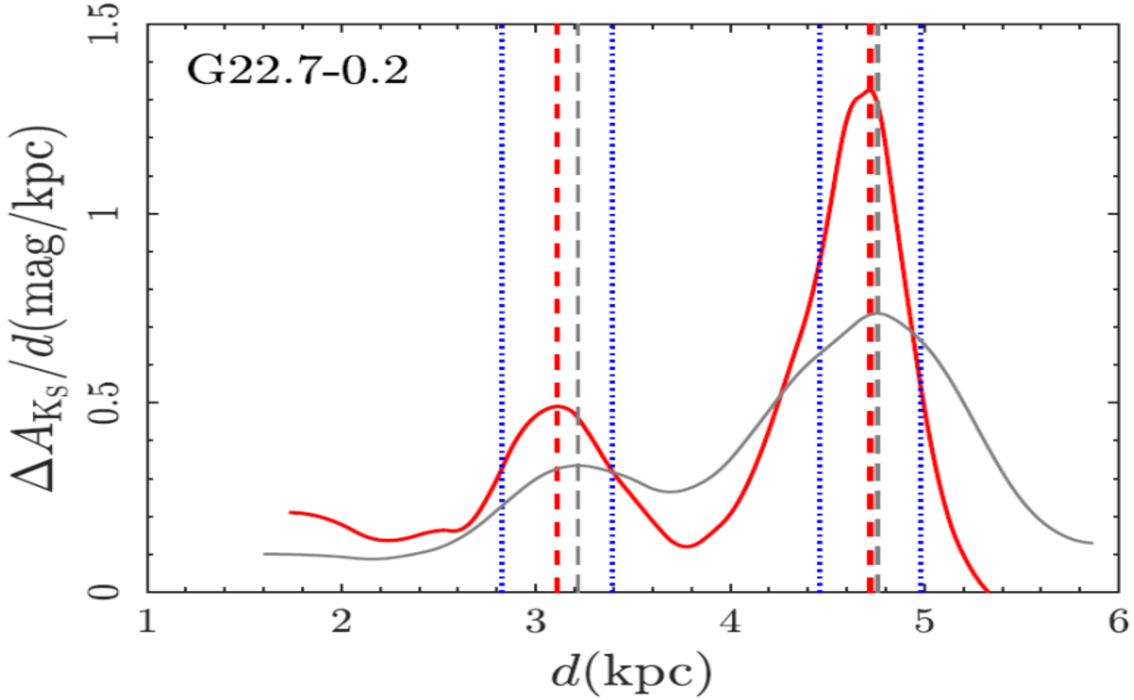

Wang+2020

Question: supernova remnants or molecular clouds?

- SNRs associated with MCs
  - Identified in literatures, e.g. Jiang+2010, Froebrich+2015
  - Level A
- Consistent with previous results, e.g. from kinematics
  - Level B
- Otherwise, Level C

Distances of SNRs in Level A

15A

SNR Names	$D_{\rm thiswork}$ (kpc)	$D_{\rm literature}$ (kpc)	Method	References
G78.2+2.1	0.98	1.7–2.6, 1.5 ± 0.4	associated object	1, 2
G89.0+4.7	2.3 ± 0.3	$1.9^{+0.3}_{-0.2}$, 0.80 ± 0.07, 1.0–1.6	RCs[a], associated object, $\Sigma - D$	3–8
G93.7–0.2	2.16 ± 0.02	1.5 ± 0.2	kinematics	9
G94.0+1.0	2.53 ± 1.08	4.5	associated object	10
G109.1–1.0	2.79 ± 0.04	3.0, 4.0 ± 0.8, 6.0	kinematics, RCs	11–13
G152.4–2.1	0.59 ± 0.09	1.1 ± 0.1, ⩽**1.0**	kinematics, extinction	14, **32**
G156.2+5.7	0.68 ± 0.20	0.3, 1–3, 1.3, 3	associated object, kinematics, Sedov estimate	15–18
G160.9+2.6	0.54 ± 0.10	0.8 ± 0.4, 1.1, 1.3–1.8, ⩾1.1, **0.6**	kinematics, Sedov estimate, $\Sigma - D$, associated object, extinction	19, 20, 7, 21, **32**
G166.0+4.3	3.24 ± 0.03	4.5 ± 1.5	kinematics	22
G182.4+4.3	1.05 ± 0.24	⩾3, ∼**1.1**	Sedov estimate, extinction	23, **32**
G189.1+3.0	1.80 ± 0.05	0.7–1.5, 1.9, 1.5, $\mathbf{1.73}^{+0.13}_{-0.09}$	kinematics, $\Sigma - D$, associated object, extinction	21, 24, 7, 8, 25, **32**
G190.9–2.2	1.03 ± 0.01	1.0 ± 0.3, $\mathbf{1.03}^{+0.02}_{-0.08}$	kinematics, extinction	26, **32**
G205.5+0.5	1.13 ± 0.01	1.6 ± 0.3, 1.6, 1.5, $\mathbf{0.93}^{+0.05}_{-0.08}/\mathbf{1.26}^{+0.09}_{-0.10}$	$\Sigma - D$, extinction	27–29, **32**
G206.9+2.3	0.89 ± 0.02	3–5, 1.6	$\Sigma - D$, kinematics	28, 30
G213.0–0.6	1.09 ± 0.29	∼1.0, 2.4, **1.15** ± 0.08	kinematics, associated object, extinction	30, 31, **32**

Distances of SNRs in Level B

7B

SNR Names	$D_{\rm thiswork}$ (kpc)	$D_{\rm literature}$ (kpc)	Method	References
G65.3+5.7	1.51 ± 0.04	0.77 ± 0.20	proper motion	1
G74.0–8.5	<1.0	0.77, $0.54^{+0.01}_{-0.008}$, 0.735 ± 0.025	kinematic, shock velocity, associated object	2–4
G82.2+5.3	1.34 ± 0.13	1.6–3.3, 1.6, 3.2 ± 0.4	Sedov estimate, expansion velocity, RCs	5–7
G108.2–0.6	1.02 ± 0.01	3.2 ± 0.6	kinematics	8
G113.0+0.2	<3.8	3.1	kinematics	9
G116.9+0.2	4.3 ± 0.2	1.6, 4.2	kinematics	10, 11
G127.1+0.5	<2.9	0.3/1.3, 1.15	associated object, kinematics	12, 13

Zhao+2020

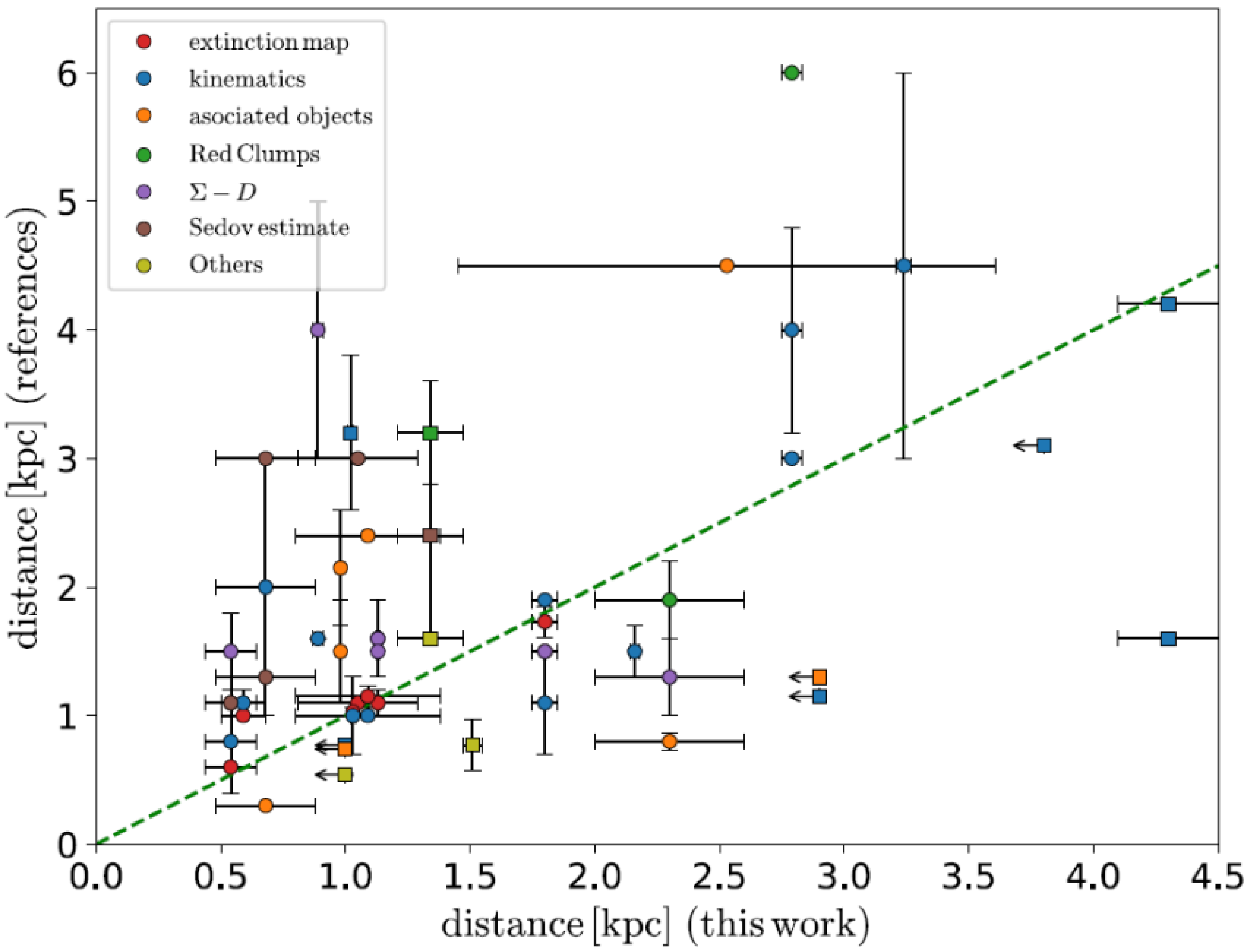

extinction map
kinematics
asociated objects
Red Clumps
$\Sigma - D$
Sedov estimate
Others
distance [kpc] (references)
distance [kpc] (this work)
0.0
0.5
1.0
1.5
2.0
2.5
3.0
3.5
4.0
4.5
0
1
2
3
4
5
6

Zhao+2020

Table 1. Distance and extinction of 35 SNRs measured by UKIDSS data.

Name [(a)]	Other name	RA (deg)	Dec (deg)	Radius (deg)	RC ridge [(b)]	$(d_{\rm ext})_{\rm P}$ [(c)] (kpc)	$(\Delta A_{K_S})_{\rm P}$ (mag kpc^{-1})	$(d_{\rm ext})_{\rm S}$ [(d)] (kpc)
G5.4-1.2[a]	Milne 56	270.54	−24.90	0.29	Normal	**3.89 ± 0.91**	0.15	0
G6.1+1.2		268.73	−23.08	0.25	Normal	**3.27 ± 0.73**	0.10	0
G6.4-0.1[a]	W28	270.13	−23.43	0.40	KDE	**3.55 ± 0.90**	0.40	0
G8.9+0.4		270.99	−21.05	0.20	KDE	**3.54 ± 0.62**	0.27	0
G13.3-1.3		274.83	−18.00	0.58	Normal	**4.76 ± 0.93**	0.10	0
G15.1-1.6		276.00	−16.57	0.25	Normal	**2.91 ± 0.68**	0.16	0
G18.9-1.1[a]		277.46	−12.97	0.28	Normal	5.47 ± 0.79	0.25	**3.08 ± 0.65**
G19.1+0.2		276.23	−12.12	0.23	Normal	**3.57 ± 0.67**	0.15	0
G21.8-0.6[a]	Kes 69	278.19	−10.13	0.17	Normal	**4.87 ± 0.29**	0.81	3.56 ± 0.24
G22.7-0.2[a]		278.31	−9.22	0.22	Normal	**4.72 ± 0.26**	1.33	3.11 ± 0.29
G23.3-0.3[a]	W41	278.69	−8.80	0.23	Normal	**3.38 ± 0.26**	1.34	4.14 ± 0.27
G24.7+0.6[a]		278.54	−7.08	0.25	Normal	**2.73 ± 0.68**	0.31	5.87 ± 0.71
G25.1-2.3		281.29	−8.00	0.67	Normal	**3.45 ± 0.83**	0.05	0
G27.8+0.6[a]		279.96	−4.40	0.42	KDE	**3.99 ± 0.55**	0.21	0
G30.7+1.0		281.00	−1.53	0.20	Normal	**3.64 ± 0.93**	0.13	0
G32.1-0.9[a]		283.29	−1.13	0.33	KDE	**4.65 ± 0.56**	0.11	0
G34.7-0.4[a]	W44, 3C392	284.00	1.37	0.29	Normal	**2.66 ± 0.71**	0.49	0
G36.6-0.7		285.15	2.93	0.21	Normal	**8.66 ± 1.17**	0.10	0
G38.7-1.3[a]		286.67	4.47	0.27	KDE	**4.11 ± 0.88**	0.08	0
G40.5-0.5[a]		286.79	6.52	0.18	KDE	**5.12 ± 0.32**	0.44	0
G42.8+0.6		286.83	9.08	0.20	KDE	**4.24 ± 0.93**	0.13	0
G43.9+1.6		286.46	10.50	0.50	KDE	**1.52 ± 0.60**	0.07	5.56 ± 0.53
G45.7-0.4		289.10	11.15	0.18	Normal	**6.04 ± 0.33**	0.31	0
G49.2-0.7[a]	W51	290.96	14.10	0.25	Normal	**5.74 ± 0.98**	0.14	0
G54.4-0.3[a]	HC40	293.33	18.93	0.33	Normal	**6.64 ± 1.25**	0.13	2.4 ± 0.63
G55.0+0.3		293.00	19.83	0.17	Normal	**10.18 ± 1.28**	0.09	6.7 ± 1.0
G59.8+1.2		294.73	24.32	0.17	Normal	**5.43 ± 1.11**	0.06	0
G65.1+0.6[a]		298.67	28.58	0.75	KDE	**4.16 ± 0.61**	0.11	0
G66.0+0.0		299.46	29.05	0.26	Normal	**3.93 ± 0.71**	0.09	0
G73.9+0.9[a]		303.56	36.20	0.23	Normal	**4.00 ± 0.69**	0.14	0
G85.4+0.7[a]		312.67	45.37	0.20	Normal	**3.80 ± 1.05**	0.08	0
G85.9-0.6		314.67	44.88	0.20	Normal	**3.27 ± 0.97**	0.05	0
G93.7-0.2	CTB 104A, DA 551	322.33	50.83	0.67	KDE	4.29 ± 0.45	0.17	**1.99 ± 0.33**
G359.0-0.9[a]		266.71	−30.27	0.19	Normal	**3.49 ± 0.36**	0.60	0
G359.1-0.5[a]		266.38	−29.95	0.20	Normal	**3.29 ± 0.47**	1.03	0

Table 2. Distance and extinction of 34 SNRs measured by VVV data.

Name [(a)]	Other name	RA (deg)	Dec (deg)	Radius (deg)	RC ridge [(b)]	$(d_{\rm ext})_{\rm P}$ [(c)] (kpc)	$(\Delta A_{K_S})_{\rm P}$ (mag kpc^{-1})	$(d_{\rm ext})_{\rm S}$ [(d)] (kpc)	$(\Delta A_{K_S})_{\rm S}$ (mag kpc^{-1})	Reliability	$d_{\rm rad}$ [(e)] (kpc)	$d_{\rm other}$ [(f)] (kpc)	$(A_{K_S})_{\rm SNR}$ (mag)	Dust mass ($M_\odot$)
G3.8+0.3		268.23	−25.47	0.15	Normal	**4.14 ± 0.29**	0.32	0	0	A	6.4		0.399	$8.25^{+3.10}_{-1.46}$
G5.4-1.2[a]	Milne 56	270.54	−24.90	0.29	Normal	**3.89 ± 0.37**	0.14	0	0	A		>4.3	0.235	$16.22^{+6.08}_{-2.86}$
G6.1+1.2		268.73	−23.08	0.25	Normal	**3.67 ± 0.36**	0.12	0	0	A	6.7		0.197	$7.71^{+2.89}_{-1.36}$
G6.4-0.1[a]	W28	270.13	−23.43	0.40	KDE	**3.55 ± 0.34**	0.56	0	0	A		1.9	0.772	$83.30^{+31.24}_{-14.70}$
G6.5-0.4		270.55	−23.57	0.15	Normal	**3.72 ± 0.21**	0.70	0	0	A	4.1		0.578	$9.60^{+3.60}_{-1.69}$
G8.7-0.1[a]	W30	271.38	−21.43	0.38	KDE	**4.15 ± 0.19**	0.62	0	0	B	1.9	4.5^	0.573	$74.37^{+27.89}_{-13.12}$
G8.9+0.4		270.99	−21.05	0.20	KDE	**3.51 ± 0.41**	0.21	0	0	A	4.3		0.338	$8.91^{+3.34}_{-1.57}$
G296.1-0.5		177.79	−62.57	0.31	KDE	**3.80 ± 0.50**	0.09	0	0	C		3.0 ± 1.0*	0.195	$9.68^{+3.63}_{-1.71}$
G301.4-1.0		189.48	−63.82	0.31	Normal	**2.74 ± 0.55**	0.12	0	0	A	5.2		0.254	$6.04^{+2.27}_{-1.07}$
G308.8-0.1		205.63	−62.38	0.25	Normal	**3.92 ± 0.60**	0.28	0	0	A		$6.9^{+8.1}_{-2.9}$*	0.885	$30.30^{+11.36}_{-5.35}$
G309.8+0.0		207.63	−62.08	0.21	Normal	**3.12 ± 0.22**	0.38	5.61 ± 0.42	0.3	A	4		0.497	$8.52^{+3.20}_{-1.50}$
G312.4-0.4[a]		213.25	−61.73	0.32	Normal	**4.41 ± 0.50**	0.25	0	0	C	2.4	>6/>14/$6.0^{+8.0}_{0.0}$*	0.600	$62.50^{+23.44}_{-11.03}$
G315.4-0.3		218.98	−60.60	0.20	Normal	**3.31 ± 0.28**	0.26	5.94 ± 0.36	0.25	C			0.351	$4.48^{+1.68}_{-0.79}$
G315.9+0.0		219.60	−60.18	0.21	KDE	**3.71 ± 0.18**	0.61	0	0	A	8.2		0.517	$9.25^{+3.47}_{-1.63}$
G316.3+0.0	MSH 14-57	220.38	−60.00	0.24	Normal	**3.84 ± 0.30**	0.55	0	0	C	4.1	>7.2/7.2 ± 0.6*	0.810	$18.04^{+6.76}_{-3.18}$
G318.2+0.1		223.71	−59.07	0.33	KDE	**3.27 ± 0.44**	0.45	0	0	A			0.870	$48.25^{+18.10}_{-8.52}$
G318.9+0.4		224.63	−58.48	0.25	Normal	**3.50 ± 0.32**	0.28	0	0	A			0.401	$7.68^{+2.88}_{-1.36}$
G320.4-1.2	MSH 15-52, RCW 89	228.63	−59.13	0.29	Normal	**3.00 ± 0.45**	0.08	5.85 ± 0.22	0.05	C		5.2	0.185	$7.58^{+2.84}_{-1.34}$
G320.6-1.6		229.46	−59.27	0.50	KDE	**3.18 ± 0.62**	0.06	0	0	C			0.150	$10.13^{+3.80}_{-1.79}$
G321.9-0.3		230.17	−57.57	0.26	KDE	**5.46 ± 0.39**	0.22	0	0	A	3.8	$6.5^{+3.5}_{-1.0}$*	0.382	$30.16^{+11.31}_{-5.32}$
G321.9-1.1		230.94	−58.22	0.23	Normal	**3.29 ± 0.75**	0.09	0	0	C			0.276	$8.69^{+3.26}_{-1.53}$
G327.1-1.1		238.60	−55.15	0.15	Normal	**4.52 ± 0.84**	0.09	0	0	A			0.310	$7.63^{+2.86}_{-1.35}$
G327.4+0.4	Kes 27	237.08	−53.82	0.18	Normal	**2.81 ± 0.16**	0.64	0	0	A	3.7	4.3–5.4	0.562	$7.30^{+2.74}_{-1.29}$
G329.7+0.4		240.33	−52.30	0.33	Normal	**2.80 ± 0.28**	0.28	0	0	A			0.464	$17.87^{+6.70}_{-3.15}$
G335.2+0.1		246.94	−48.78	0.18	Normal	**3.91 ± 0.49**	0.49	0	0	C	4.2	1.8*	1.035	$25.95^{+9.73}_{-4.58}$
G341.2+0.9		251.90	−43.78	0.18	KDE	**4.30 ± 0.43**	0.28	0	0	A			0.544	$13.17^{+4.94}_{-2.32}$
G343.1-0.7		255.10	−43.23	0.23	KDE	**3.11 ± 0.22**	0.86	0	0	A	4.5		0.835	$17.02^{+6.38}_{-3.00}$
G347.3-0.5[a]	RX J1713.7-3946	258.46	−39.75	0.54	KDE	**4.56 ± 0.58**	0.09	0	0	B		1.3†/6 ± 1∨	0.216	$59.66^{+22.37}_{-10.53}$
G351.7+0.8		260.25	−35.45	0.15	Normal	**3.35 ± 0.11**	0.64	0	0	A	5.4	13.2 ± 0.5*	0.323	$3.38^{+1.27}_{-0.60}$
G353.6-0.7		263.00	−34.73	0.25	Normal	**3.49 ± 0.22**	0.35	0	0	A	4.9	3.2+	0.388	$15.83^{+5.93}_{-2.79}$
G355.4+0.7		262.83	−32.43	0.21	Normal	**4.16 ± 0.32**	0.36	0	0	A	4.8		0.526	$21.16^{+7.93}_{-3.73}$
G357.7+0.3[a]		264.65	−30.73	0.20	KDE	**3.79 ± 0.21**	0.66	0	0	B	4.2			
G359.0-0.9[a]		266.71	−30.27	0.19	Normal	**3.29 ± 0.20**	0.96	0	0	A	3.7			
G359.1-0.5[a]		266.38	−29.95	0.20	Normal	**3.18 ± 0.32**	0.81	0	0	B	4			

34A
9B

Wang+2020

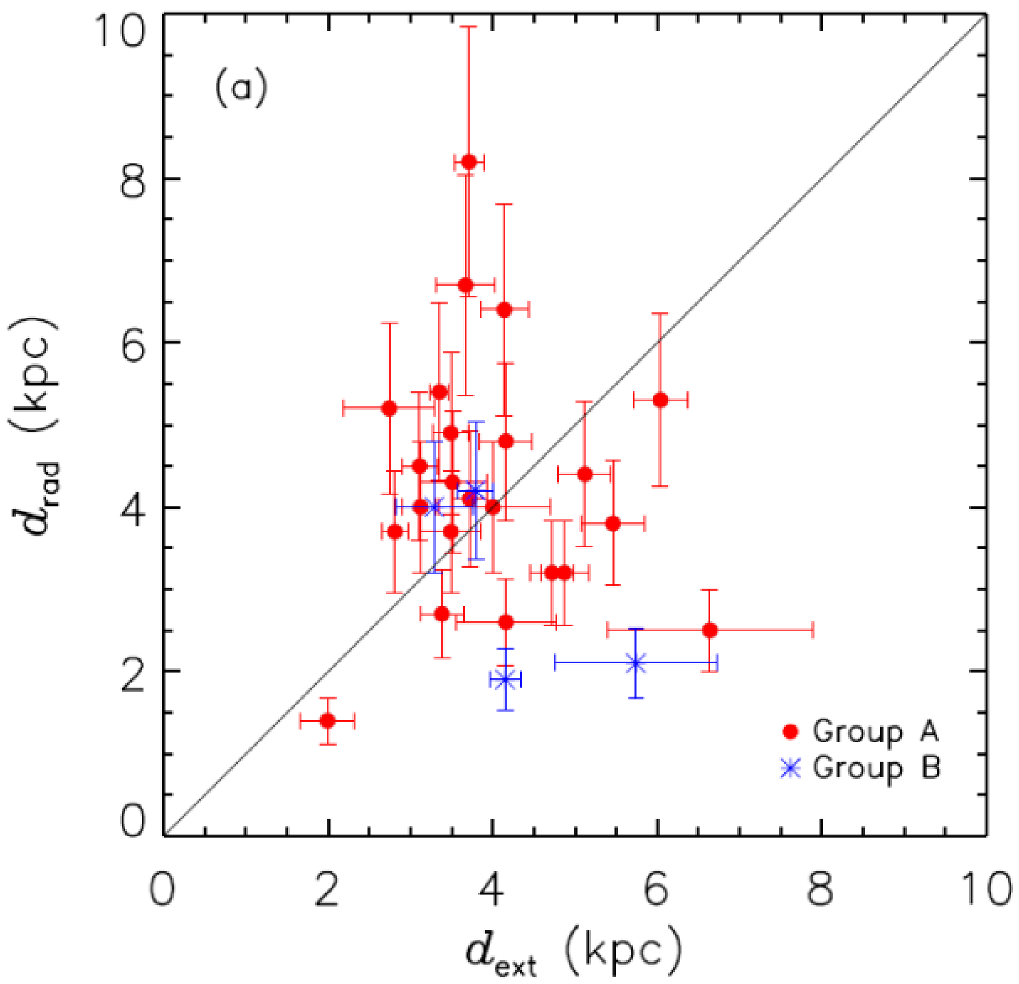

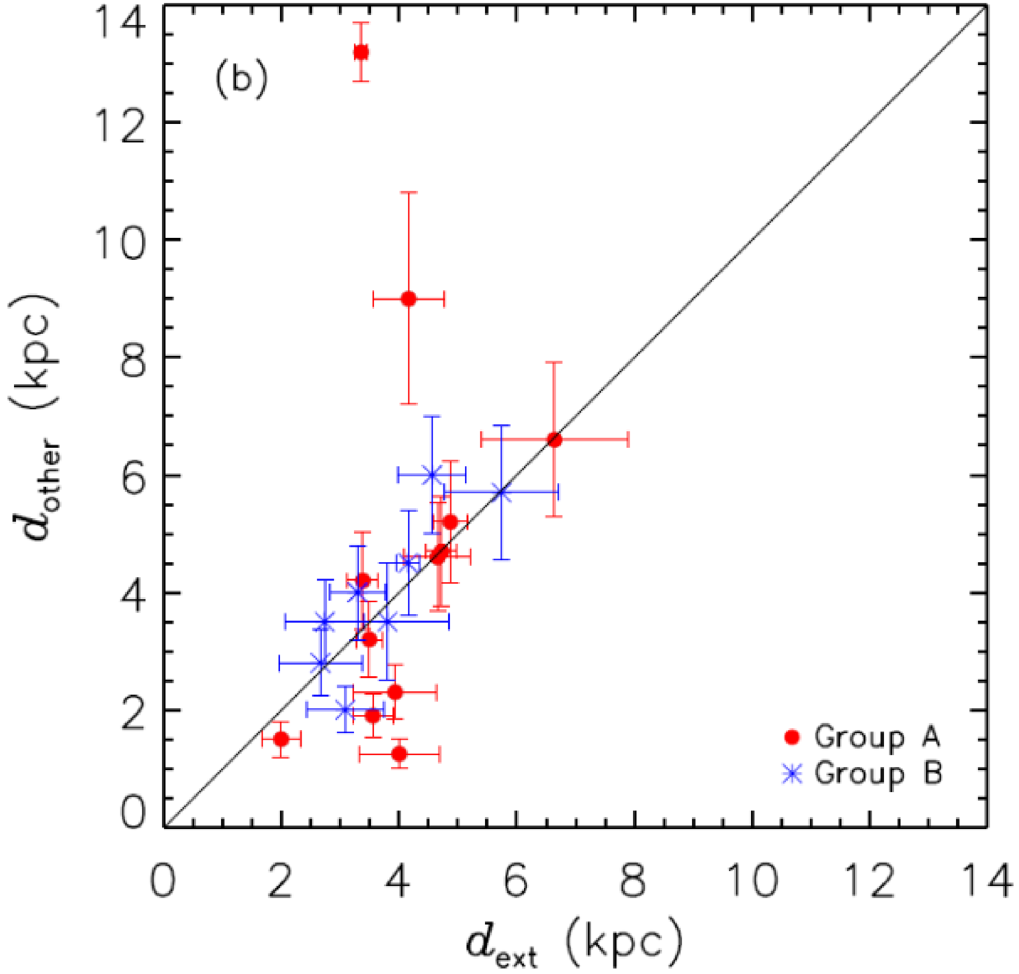

Comparison of the extinction distance with the radio-surface-brightness distance (left) of 27 SNRs, and the distances obtained by other methods (right) of 20 SNRs.

Wang+2020

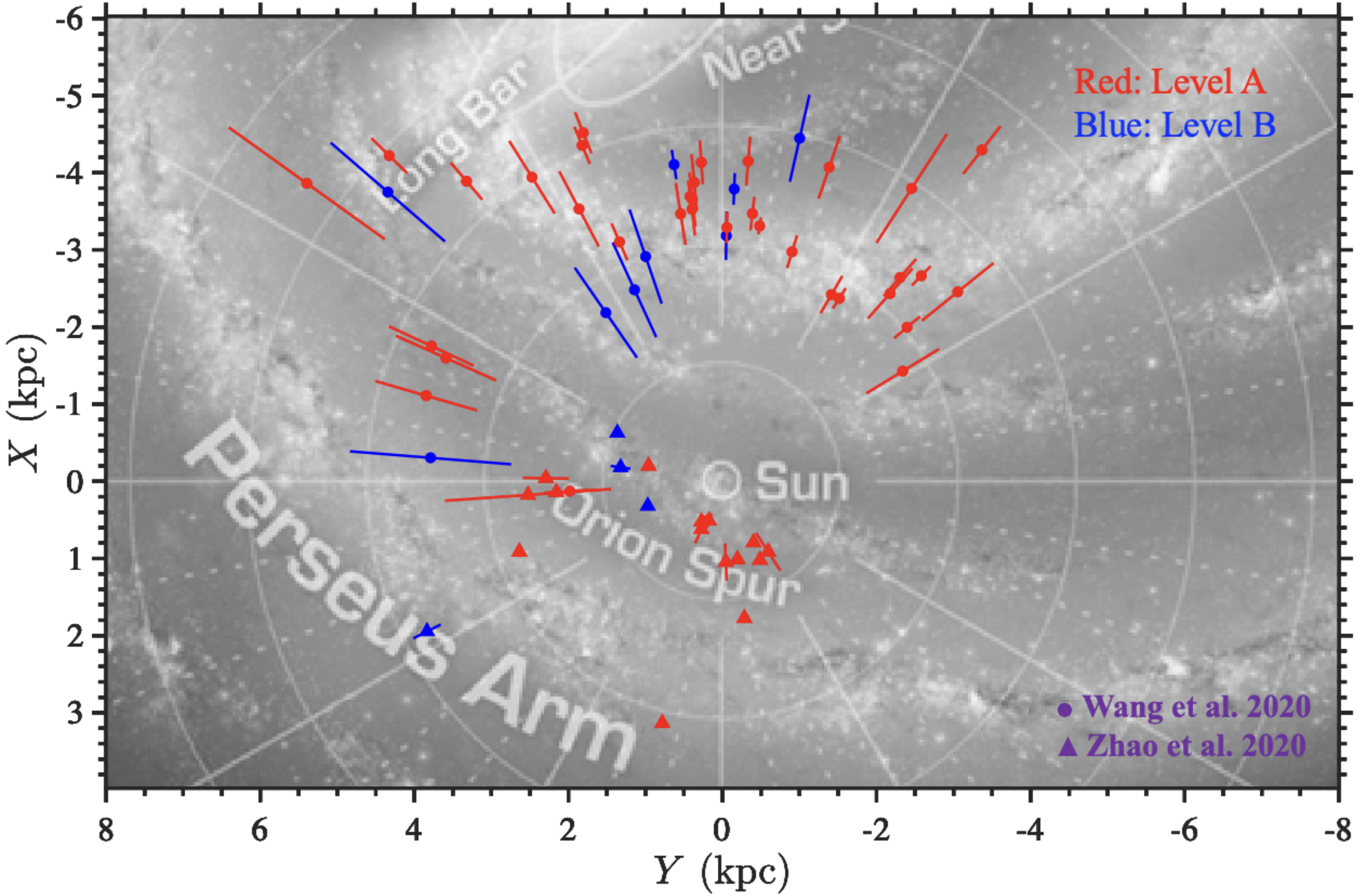

Distribution of the 64 SNRs consisted of 34+15 in Group A (red) and 9+7 in Group B (blue), respectively in the disk superimposed on the Robert Hurt’s sketch of our

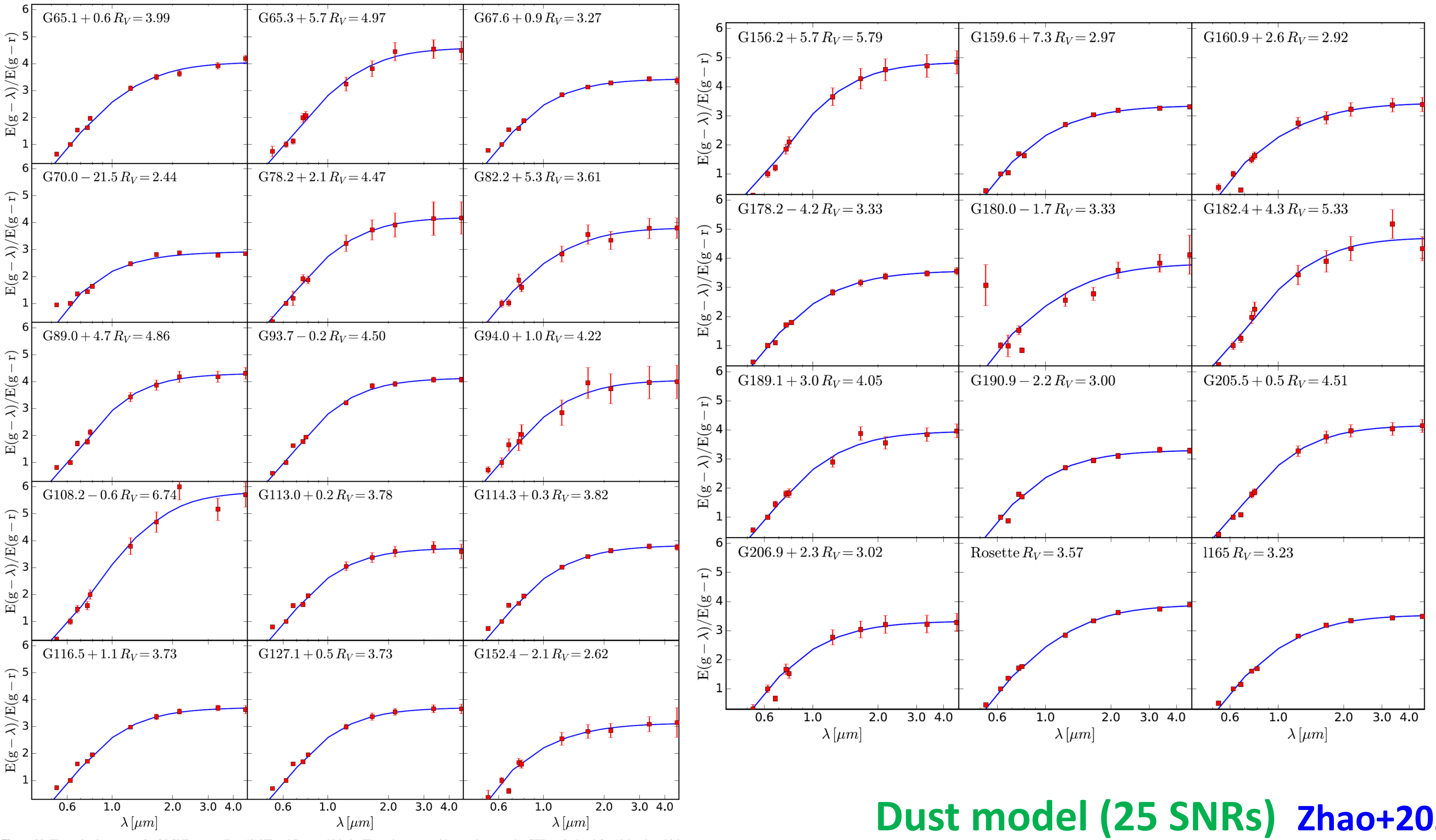

Figure 11. The extinction curves for 25 SNRs, as well as "$l165$" and Rosette Nebula. The red squares with error bars are the CERs calculated for 10 bands, which from right to left are G_{BP}, r_{P1}, G, i_{P1}, G_{RP}, J, H, K_S, W_1, and W_2, respectively. The blue lines are the best-fit results of our dust model.

Dust model (25 SNRs) **Zhao+2020**

Dust properties

- Fitting the extinction curve from about 0.6μm to 4.5μm
  - Gaia, Pan-STARRS1, 2MASS, WISE
- Model
  - graphite and silicate
  - Msil/Mgra = 2:1.
  - MRN size distribution $n(a) \propto a^{-\alpha}$
- CCM89
- 22 SNRs (Level A+B)

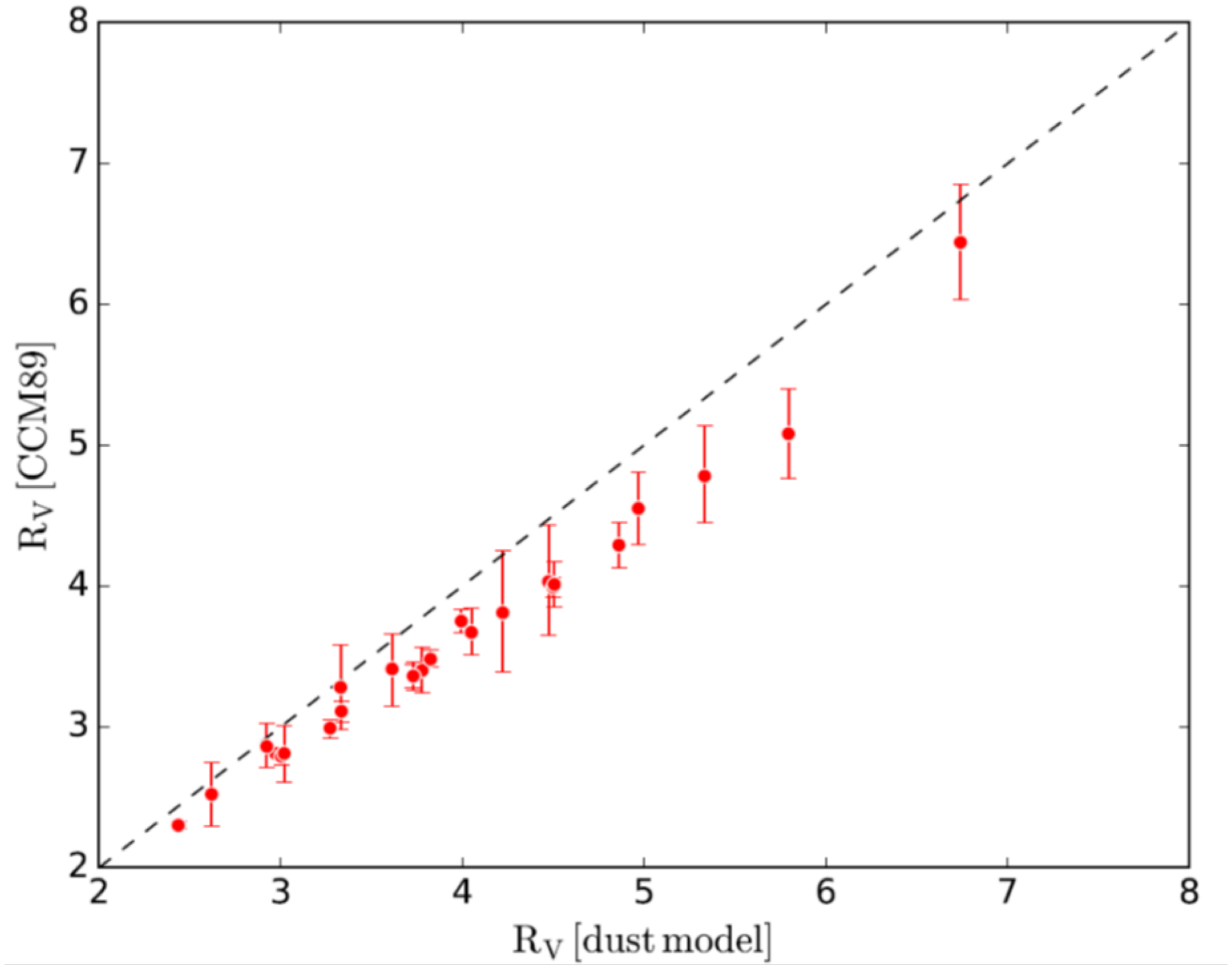

Zhao+2020

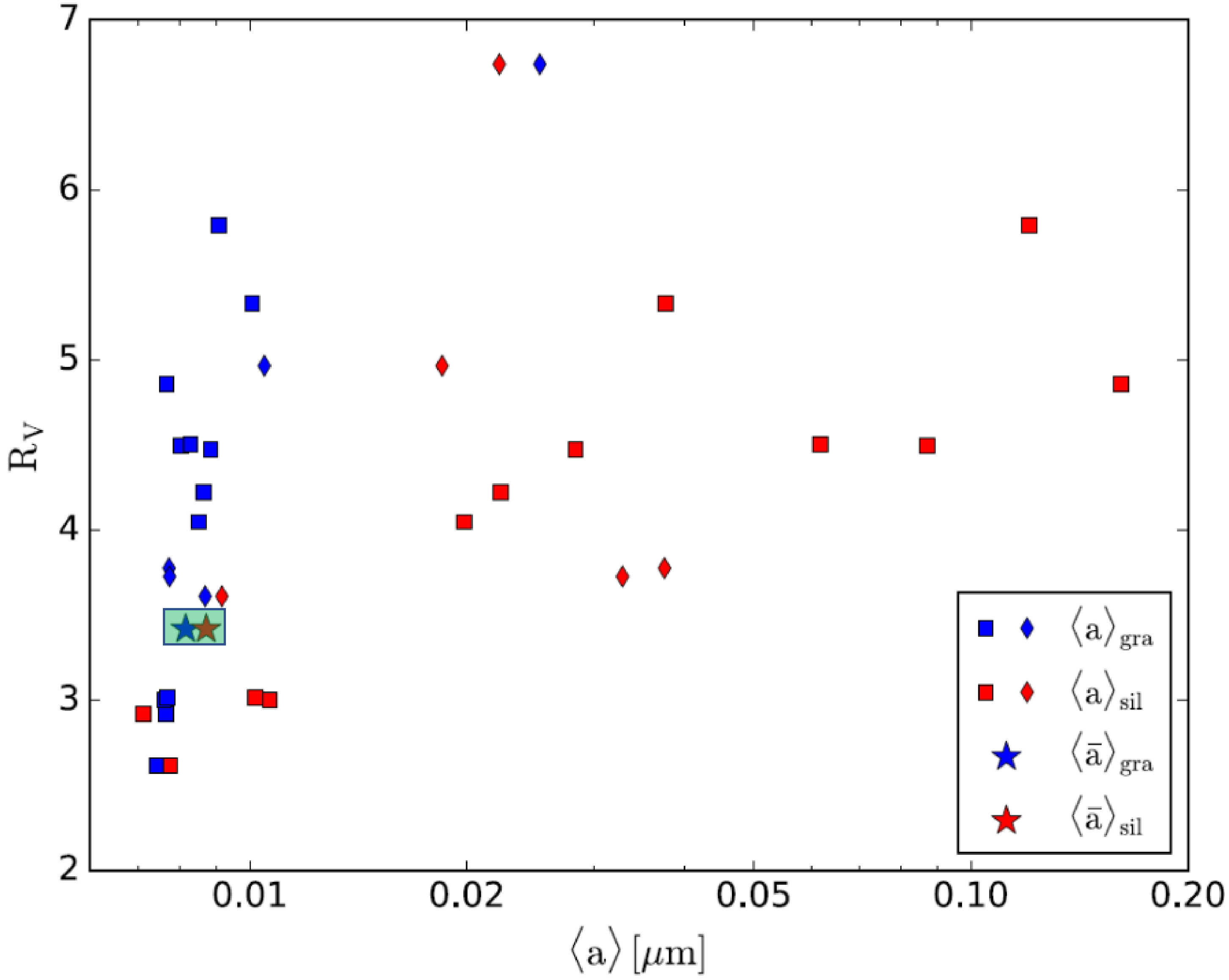

$$\langle a \rangle = \frac{\int_{a_{min}}^{a_{max}} a \cdot n(a) da}{\int_{a_{min}}^{a_{max}} n(a) da}$$

- R_V ranges from about 2.4 to 6.7
- $\langle a \rangle_{graphite}$ ~0.008 μm comparable to the diffuse ISM
- $\langle a \rangle_{silicate}$ ~ 0.02–0.03 μm, significantly bigger than the diffuse ISM
- Nozawa et al. (2007) suggested that silicate dust is more easily destroyed by SN explosion than carbonaceous dust

Zhao+2020

Dust mass from extinction

$$K_{\mathrm{ext},V} = \frac{A_V}{\Sigma_{\mathrm{dust}}} = 2.8\times10^4 \mathrm{mag\ cm^2 g^{-1}}$$ (WD01)

$$M_{\mathrm{dust}} = \frac{A_V \times \pi(R_{\mathrm{out}}^2 - R_{\mathrm{in}}^2)\times F_{\mathrm{fill}}}{K_{ext,V}}$$

$A_V = \frac{A_{Ks}}{0.11}$ (WD01) & F_{fill}=0.1 (Owen & Barlow 2015)

$$\frac{M_{\mathrm{dust}}}{\mathrm{M}_\odot} = 0.488\,\frac{A_{K_s}}{\mathrm{mag}}\left[\left(\frac{R_{\mathrm{out}}}{\mathrm{pc}}\right)^2 - \left(\frac{R_{\mathrm{in}}}{\mathrm{pc}}\right)^2\right]$$

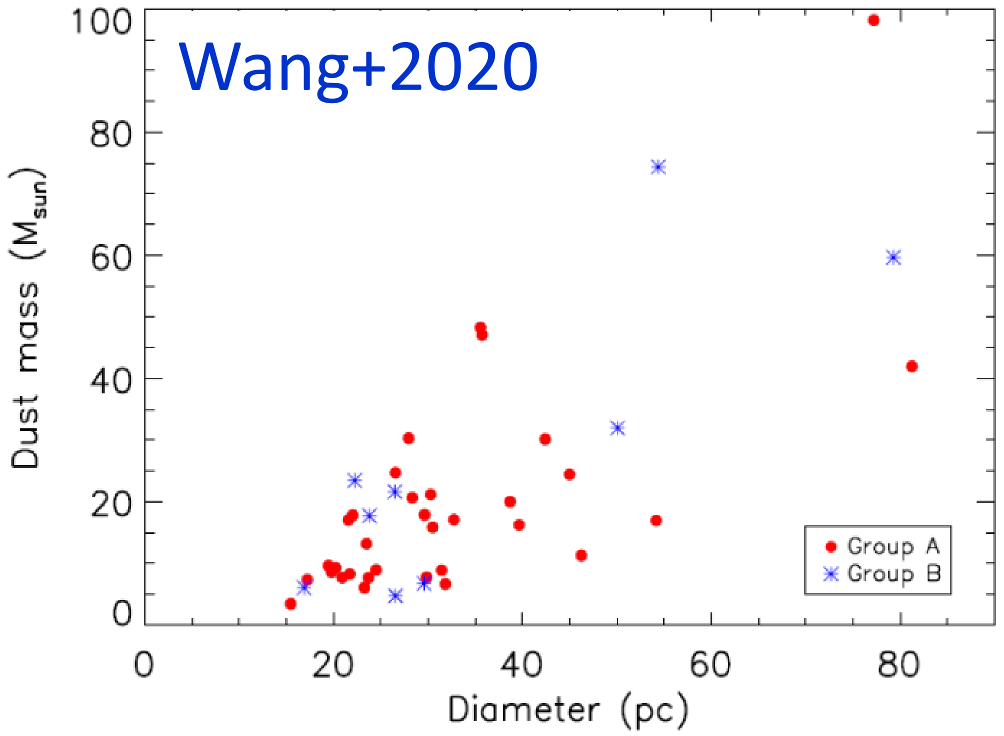

IC443 (Li+2022)

$$F_\nu(\lambda) = \frac{M_w}{d^2}\kappa(a,\lambda)B_\nu(\lambda,T_w) + \frac{M_c}{d^2}\kappa(a,\lambda)B_\nu(\lambda,T_c) \rightarrow \begin{cases} M_w \sim 0.1\mathrm{M}_\odot @ T_w \sim 53K \\ M_c \sim 46\mathrm{M}_\odot @ T_c \sim 17K \end{cases}$$

M_{dust}^{ext}: ~ 66$\mathrm{M}_\odot$ from the visual extinction

Summary

- The distances and extinctions with high accuracy are determined for
  - 22 (+10) Zhao+2020
  - 43 (+20) Wang+2020
  - 4 (+3) Yu+2019
  - **22+43(-1)+4(-4)=64 Galactic SNRs from their sharp increase of extinction**
  - **7 for the first time**
- The extinction law is determined towards 22 SNRs, found to have bigger total-to-selective extinction ratio (R_V)
- The size of silicate dust in SNRs is found to be bigger than in the diffuse ISM, which agrees with the model result
- The dust mass is estimated for the SNR in Wang+2020, ranging from several to a few tens solar mass

To be done

- Improvement of the method
  - Distance-sliced extinction and CO map
    - Morphological agreement
- Application to more SNRs
  - Optically too thin/thick SNR
    - Ultraviolet/infrared bands
  - JWST data for distant/high extinction SNRs

IC443

Variation of E(B-V) with distance at several clumps

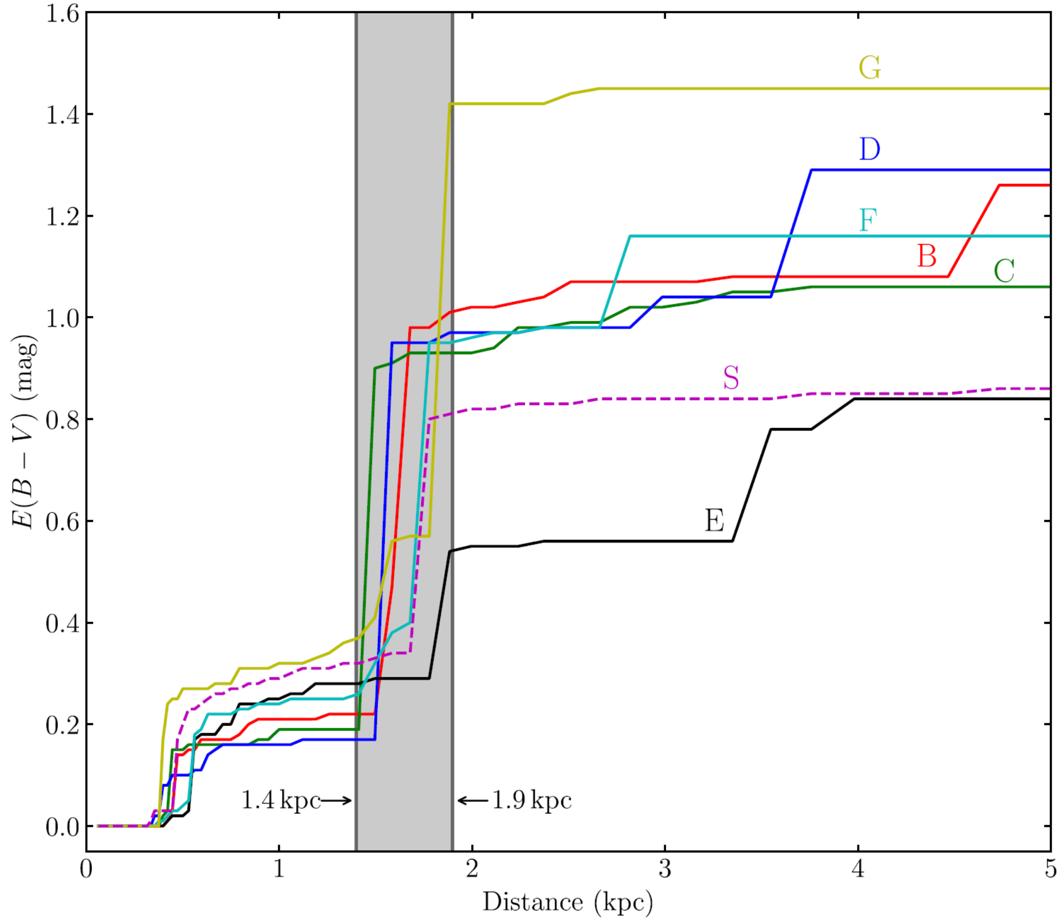

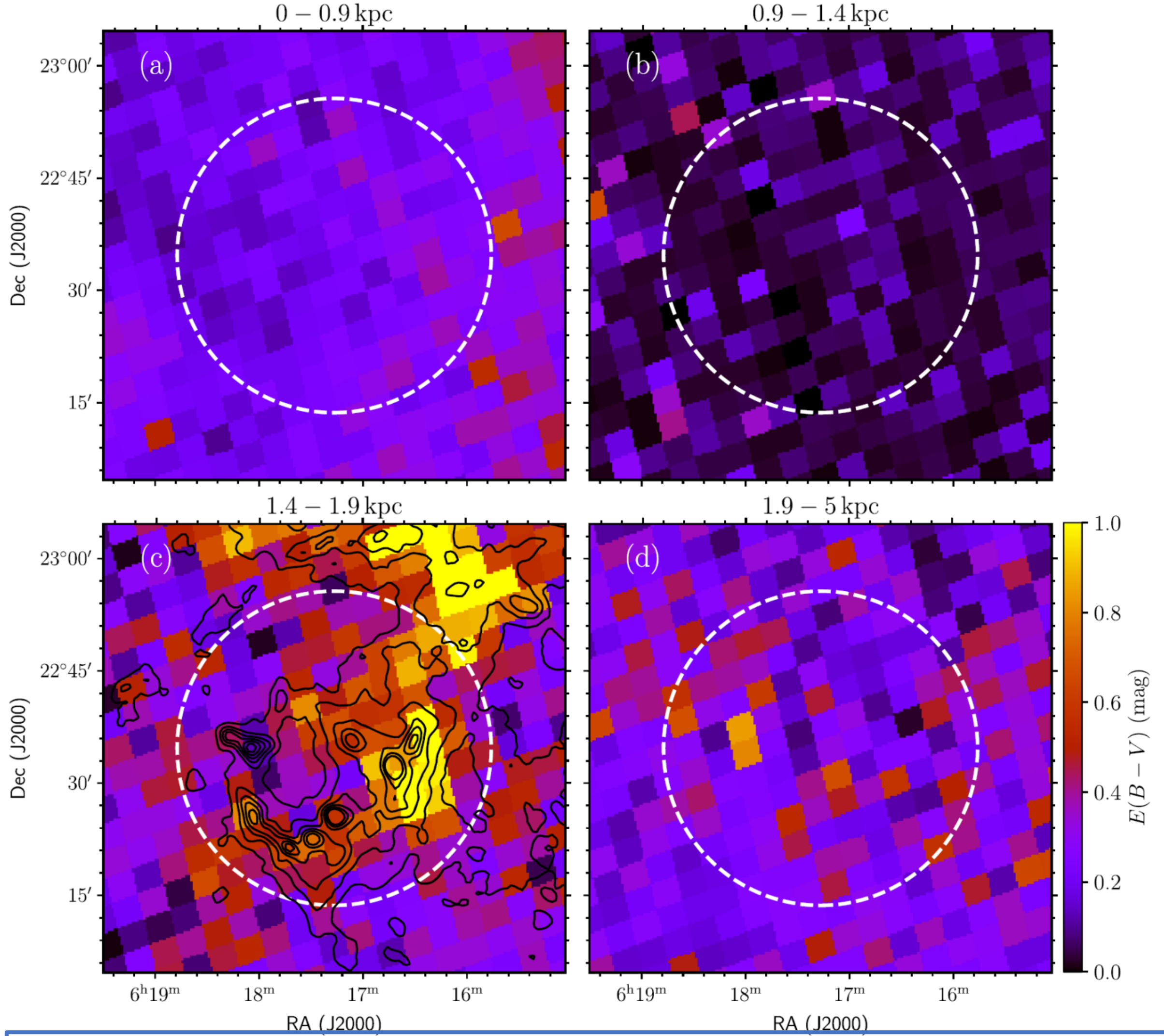

Sliced extinction map at four distance intervals
Comparison with the CO intensity map (c)

Li+2022

Poster S6.12 Zhe Zhang

Estimation of the Dust Mass with Infrared Emission and Extinction of the Supernova Remnants: G156.2+5.7, G109.1-1.0, G166.0+4.3, G93.7-0.2

Thank you

1. Consistent in 3-8um, flat
2. Smaller than others
3. Agree with Rv=5.5 (WD01)

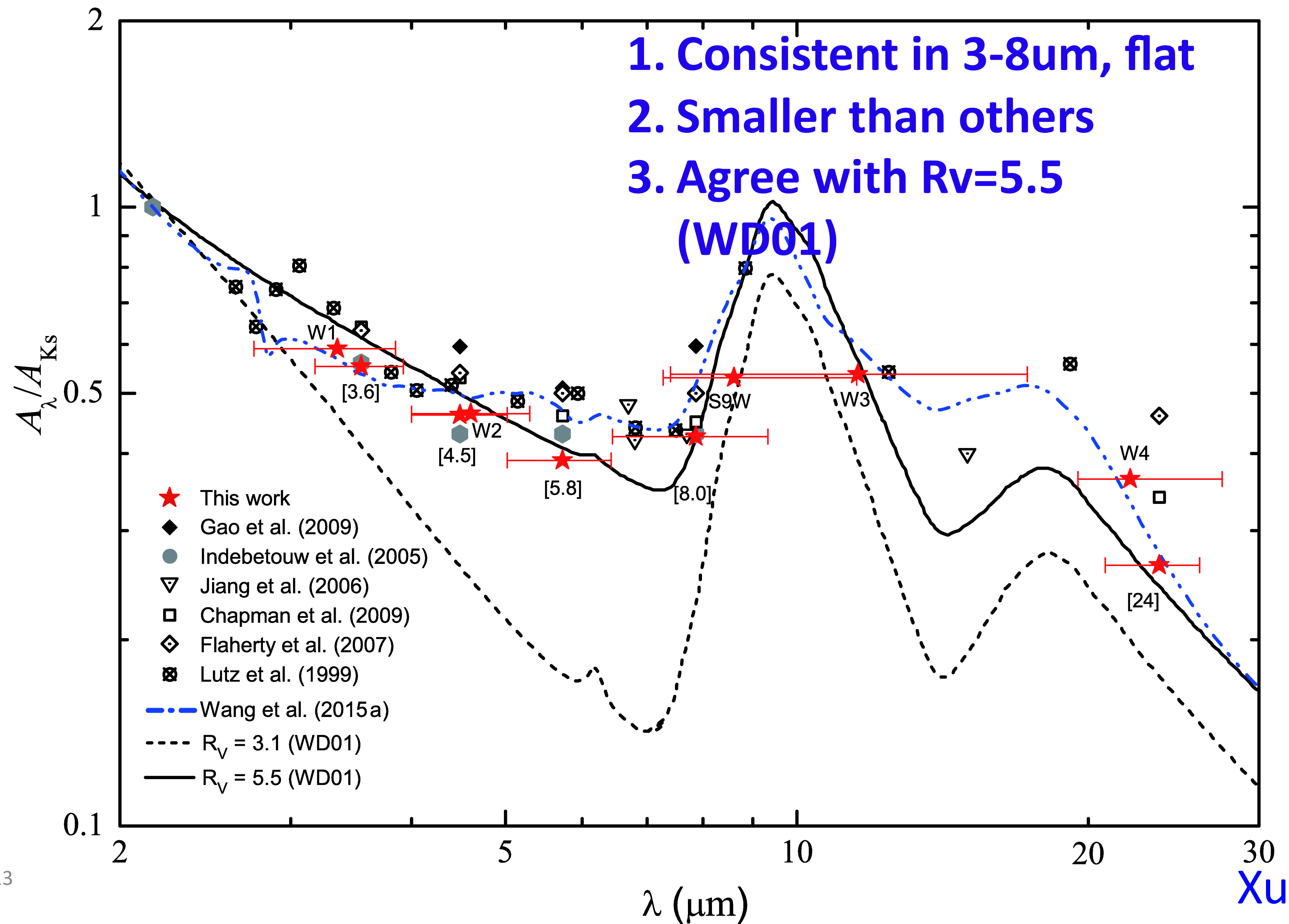

Xue+2016

Part II: Distances to the Supernova Remnants

The extinction distance

- Basic principle
  - At the position of a SNR, where the extinction increases sharply due to its higher dust density than the average foreground ISM
  - With the known extinction of a target → its distance can be derived by measuring the distribution of extinction along the distance towards the sightline.
    - the distance to the neutron star in 4U 1608-52 by Güver et al. (2010)
- Advantage
  - Applicable to almost all the SNRs
  - Apparent improvement on the precision

Region of SNR and stars superposed on the radio image

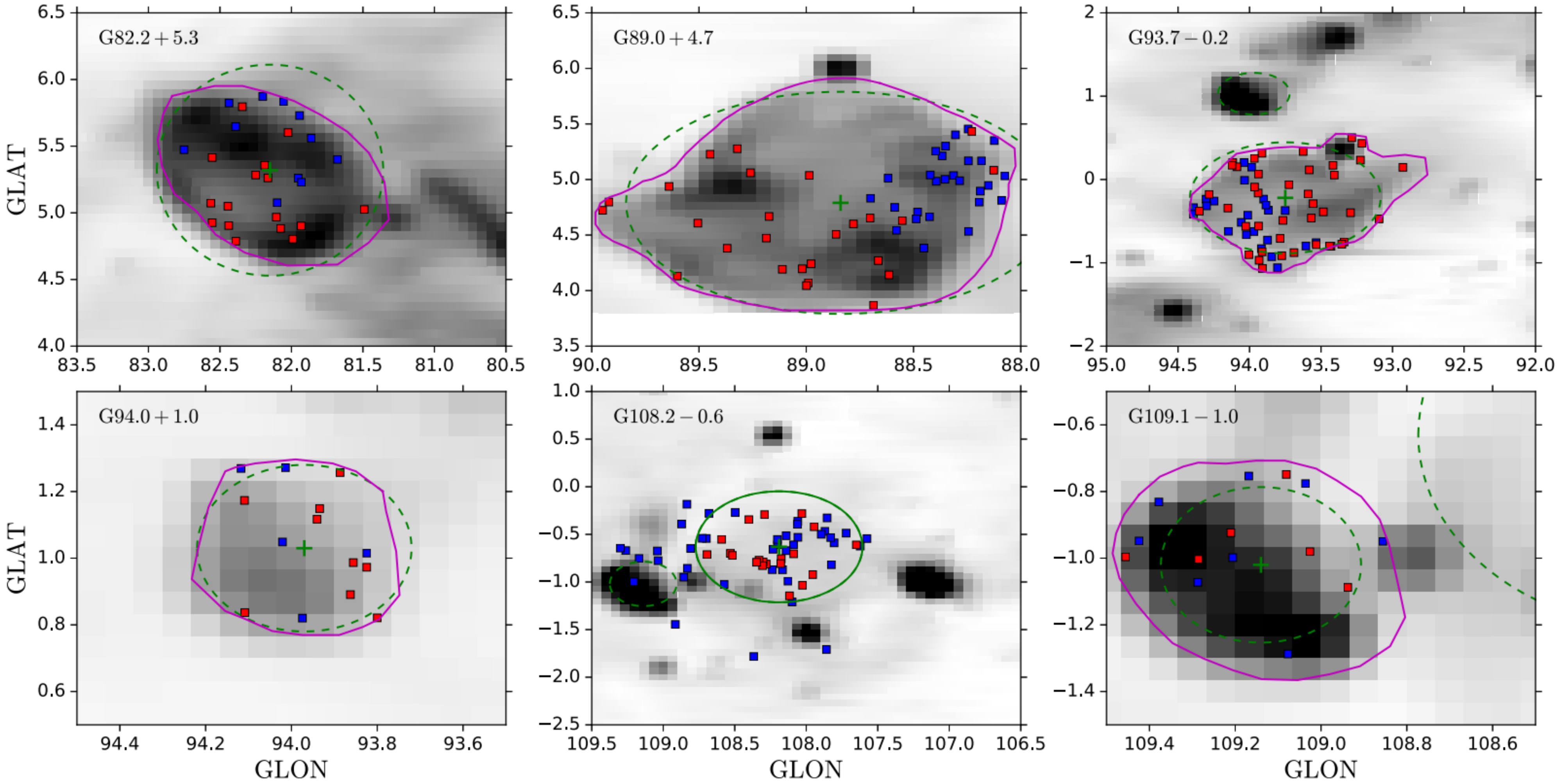

Figure 5. The selected stars and the SNR regions. The background gray image is the radio map. The green dashed circles represent the reference regions of SNRs from Green (2019), with green crosses indicating the centers. If the referred regions are used, they will be in solid lines. The magenta solid lines are manually defined regions, which follow some contour lines enclosing the SNRs. The blue and red squares denote the dwarfs and giants, respectively. All of the subpanels are in Galactic coordinates.

Extinction along/and distance

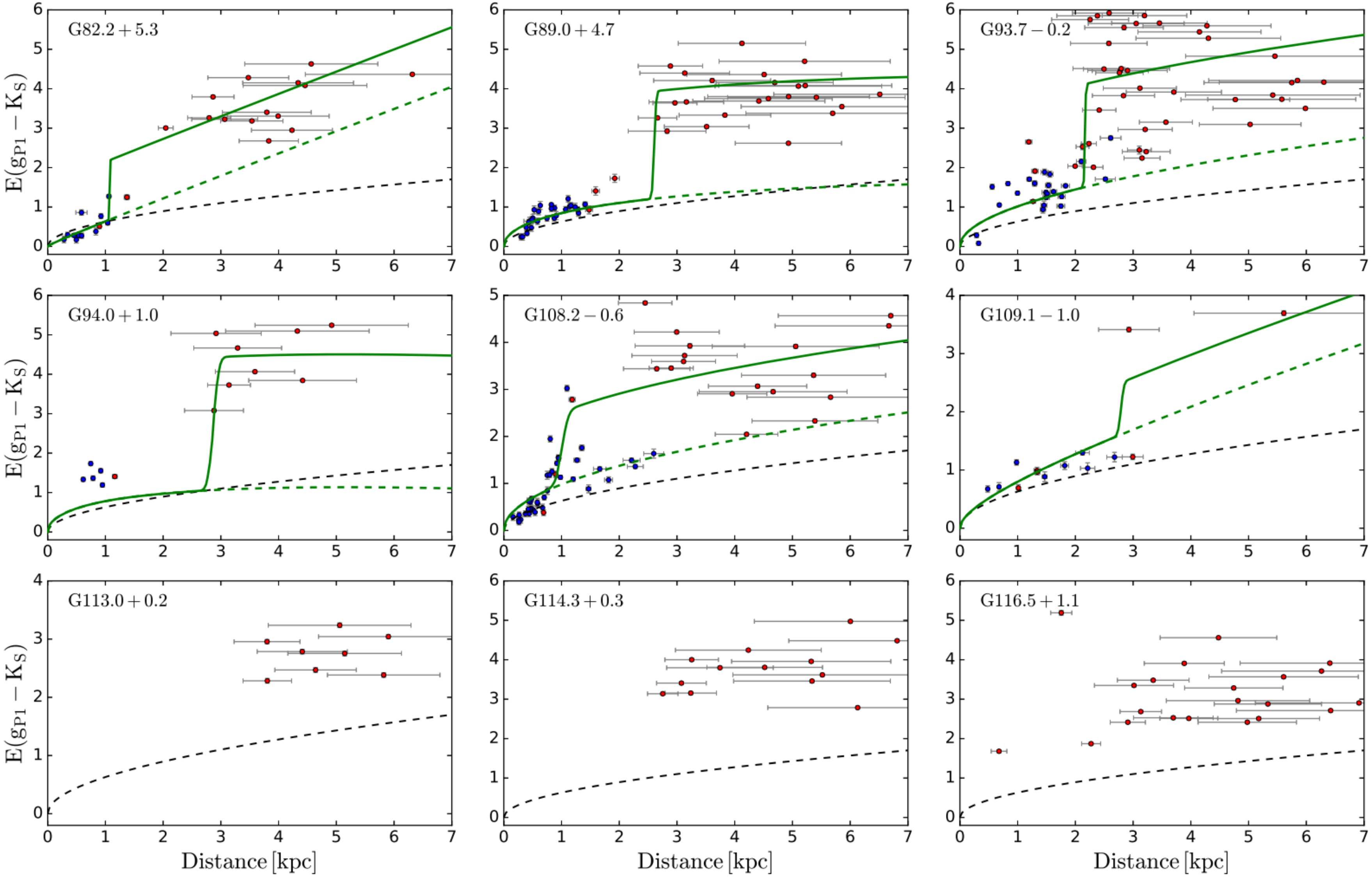

Figure 6. Color excess values $E(g_{P1} - K_S)$ vs. distances (in kpc) in the selected regions for all 32 SNRs. The blue and red dots represent dwarf and giant stars, respectively. The black dashed line is the derived common ISM reddening profile from the 118 region. The green solid lines are the best-fitting reddening profiles based on the sample stars. The green dashed lines decodes the ISM contribution derived from the extinction-distance model.

Comparison with Green et al. (2019)

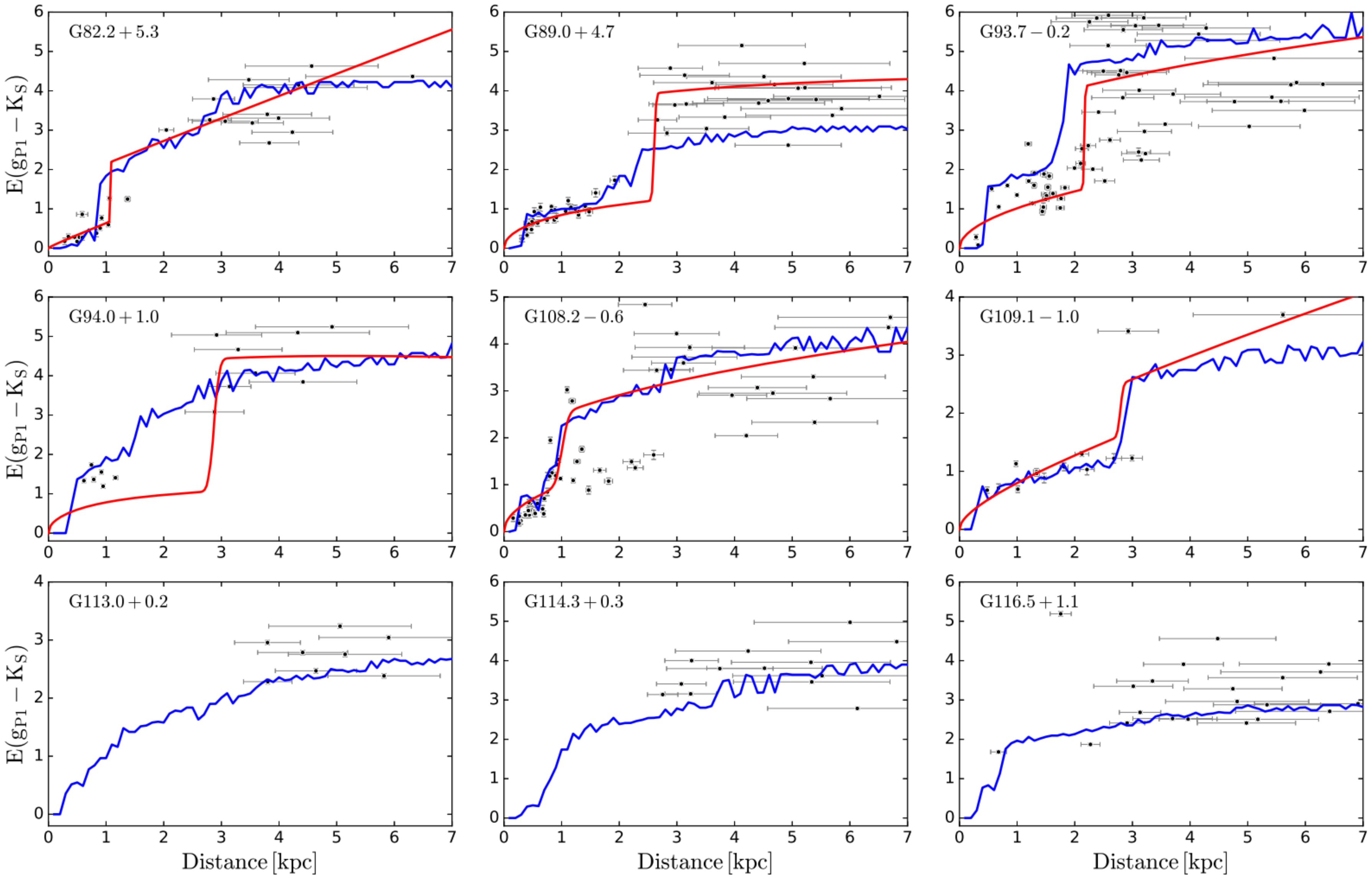

Figure 7. The comparison between our results (black dots and red lines) and the reddening profiles (blue lines) retrieved from the dust map by Green et al. (2019). The black dots and red lines are the same as the blue/red dots and green lines in Figure 6, respectively.

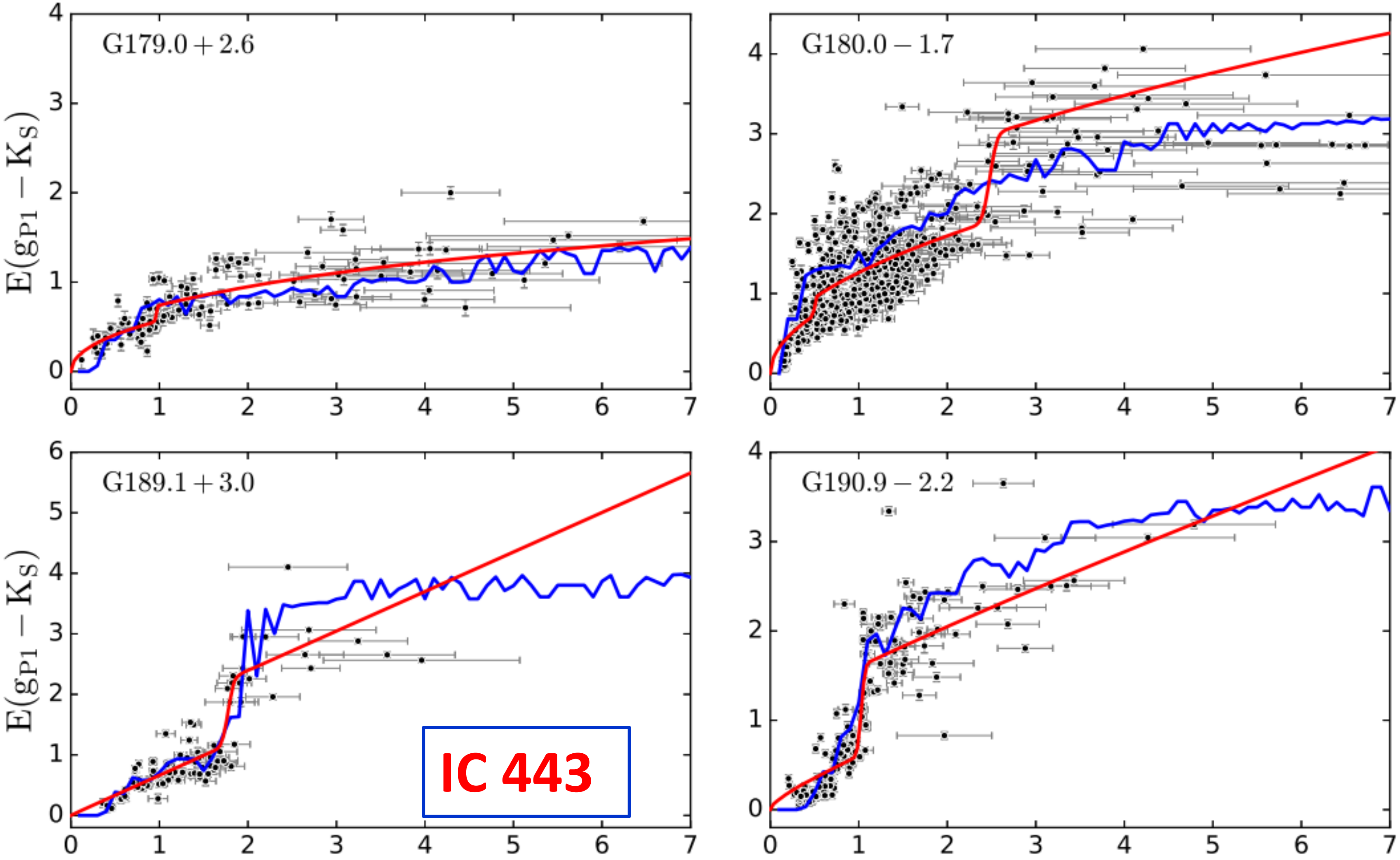

G179.0 + 2.6
G180.0 − 1.7
G189.1 + 3.0
G190.9 − 2.2
E(g_P1 − K_S)
E(g_P1 − K_S)
IC 443

Examination

- Potential risk: the extinction jump could be made by any molecular cloud in the sightline other than the supernova remnant itself
- Confirmation
  - Association with MC by references (Zhao et al. 2020)
  - Comparison with radio maps (Yu et al. 2019)
  - Comparison with surrounding regions (Wang et al. 2020)

The Monoceros SNR: jumps at ~1.0 kpc and ~2.2 kpc

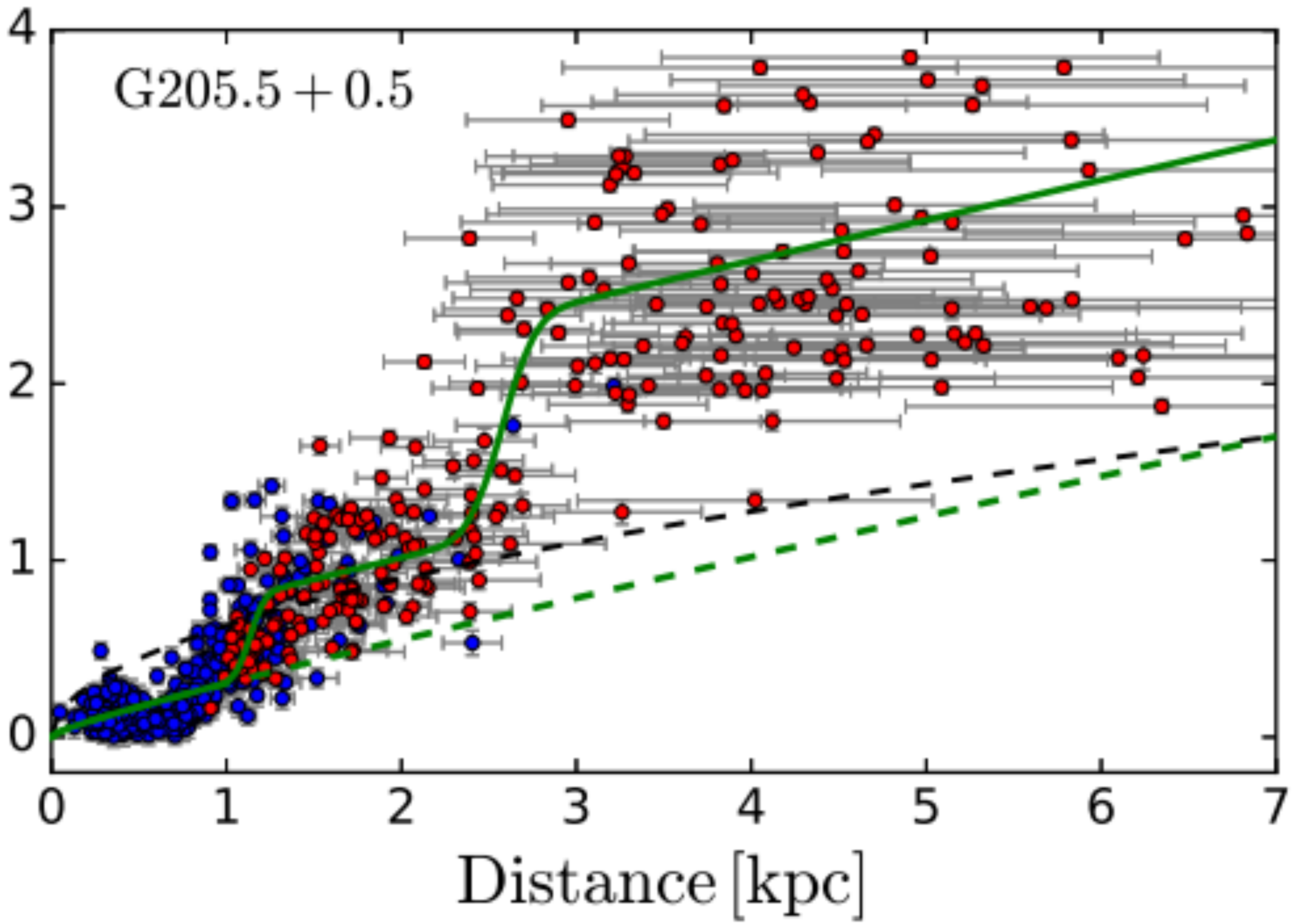

Distance

SNR Names	$D_{thiswork}$ (kpc)	$D_{literature}$ (kpc)	Method
G78.2+2.1	0.98	1.7–2.6, 1.5 ± 0.4	associated object
G89.0+4.7	2.3 ± 0.3	$1.9^{+0.3}_{-0.2}$, 0.80 ± 0.07, 1.0–1.6	RCs[a], associated object, $\Sigma - D$
G93.7–0.2	2.16 ± 0.02	1.5 ± 0.2	kinematics
G94.0+1.0	2.53 ± 1.08	4.5	associated object
G109.1–1.0	2.79 ± 0.04	3.0, 4.0 ± 0.8, 6.0	kinematics, RCs
G152.4–2.1	0.59 ± 0.09	1.1 ± 0.1, $\leqslant$**1.0**	kinematics, extinction
G156.2+5.7	0.68 ± 0.20	0.3, 1–3, 1.3, 3	associated object, kinematics, Sedov estimate
G160.9+2.6	0.54 ± 0.10	0.8 ± 0.4, 1.1, 1.3–1.8, $\geqslant$1.1, **0.6**	kinematics, Sedov estimate, $\Sigma - D$, associated object, extinction
G166.0+4.3	3.24 ± 0.03	4.5 ± 1.5	kinematics
G182.4+4.3	1.05 ± 0.24	$\geqslant$3, $\sim$**1.1**	Sedov estimate, extinction
G189.1+3.0	1.80 ± 0.05	0.7–1.5, 1.9, 1.5, $\mathbf{1.73}^{+0.13}_{-0.09}$	kinematics, $\Sigma - D$, associated object, extinction
G190.9–2.2	1.03 ± 0.01	1.0 ± 0.3, $\mathbf{1.03}^{+0.02}_{-0.08}$	kinematics, extinction
G205.5+0.5	1.13 ± 0.01	1.6 ± 0.3, 1.6, 1.5, $\mathbf{0.93}^{+0.05}_{-0.08}/\mathbf{1.26}^{+0.09}_{-0.10}$	$\Sigma - D$, extinction
G206.9+2.3	0.89 ± 0.02	3–5, 1.6	$\Sigma - D$, kinematics
G213.0–0.6	1.09 ± 0.29	$\sim$1.0, 2.4, **1.15** ± 0.08	kinematics, associated object, extinction

Distance and extinction of 35 SNRs measured by UKIDSS data

Based on the red clump stars identified in the J-K/K diagram

Table 1. Distance and extinction of 35 SNRs measured by UKIDSS data.

Name [(a)]	Other name	RA (deg)	Dec (deg)	Radius (deg)	RC ridge [(b)]	$(d_{\rm ext})_{\rm P}$ [(c)] (kpc)	$(\Delta A_{K_S})_{\rm P}$ (mag kpc^{-1})	$(d_{\rm ext})_{\rm S}$ [(d)] (kpc)	$(\Delta A_{K_S})_{\rm S}$ (mag kpc^{-1})	Reliability	$d_{\rm rad}$ [(e)] (kpc)	$d_{\rm other}$ [(f)] (kpc)	$(A_{K_S})_{\rm SNR}$ (mag)	Dust mass ($M_\odot$)
G5.4-1.2[a]	Milne 56	270.54	−24.90	0.29	Normal	**3.89 ± 0.91**	0.15	0	0	A		>4.3	0.275	$18.94^{+7.10}_{-3.34}$
G6.1+1.2		268.73	−23.08	0.25	Normal	**3.27 ± 0.73**	0.10	0	0	A	6.7		0.138	$4.27^{+1.60}_{-0.75}$
G6.4-0.1[a]	W28	270.13	−23.43	0.40	KDE	**3.55 ± 0.90**	0.40	0	0	A		1.9	0.742	$79.96^{+29.98}_{-14.11}$
G8.9+0.4		270.99	−21.05	0.20	KDE	**3.54 ± 0.62**	0.27	0	0	A	4.3		0.376	$10.06^{+3.77}_{-1.78}$
G13.3-1.3		274.83	−18.00	0.58	Normal	**4.76 ± 0.93**	0.10	0	0	C		2.0–4.0	0.214	$50.65^{+18.99}_{-8.94}$
G15.1-1.6		276.00	−16.57	0.25	Normal	**2.91 ± 0.68**	0.16	0	0	C	4.5	$2.2^{\triangleleft}$	0.186	$4.21^{+1.58}_{-0.74}$
G18.9-1.1[a]		277.46	−12.97	0.28	Normal	5.47 ± 0.79	0.25	**3.08 ± 0.65**	0.13	B		$1.8^{\star}/2.0^{\diamond}$	0.175	$6.70^{+2.51}_{-1.18}$
G19.1+0.2		276.23	−12.12	0.23	Normal	**3.57 ± 0.67**	0.15	0	0	C	4.0		0.269	$9.29^{+3.48}_{-1.64}$
G21.8-0.6[a]	Kes 69	278.19	−10.13	0.17	Normal	**4.87 ± 0.29**	0.81	3.56 ± 0.24	0.4	A	3.2	$5.2^{\circ}/5.6^{\bullet}$	0.586	$20.64^{+7.74}_{-3.64}$
G22.7-0.2[a]		278.31	−9.22	0.22	Normal	**4.72 ± 0.26**	1.33	3.11 ± 0.29	0.49	A	3.2	$4.4/4.7^{\bullet}$	0.841	$47.09^{+17.66}_{-8.31}$
G23.3-0.3[a]	W41	278.69	−8.80	0.23	Normal	**3.38 ± 0.26**	1.34	4.14 ± 0.27	0.93	A	2.7	$4.2^{\circ}/4.8^{\bullet}$	0.799	$24.70^{+9.26}_{-4.36}$
G24.7+0.6[a]		278.54	−7.08	0.25	Normal	**2.73 ± 0.68**	0.31	5.87 ± 0.71	0.26	B		$3.5^{\diamond}$	0.483	$6.03^{+2.26}_{-1.06}$
G25.1-2.3		281.29	−8.00	0.67	Normal	**3.45 ± 0.83**	0.05	0	0	C		2.9	0.100	$10.66^{+4.00}_{-1.88}$
G27.8+0.6[a]		279.96	−4.40	0.42	KDE	**3.99 ± 0.55**	0.21	0	0	A		$2–3^{\oslash}$	0.275	$24.43^{+9.16}_{-4.31}$
G30.7+1.0		281.00	−1.53	0.20	Normal	**3.64 ± 0.93**	0.13	0	0	C	5.1		0.242	$5.16^{+1.93}_{-0.91}$
G32.1-0.9[a]		283.29	−1.13	0.33	KDE	**4.65 ± 0.56**	0.11	0	0	A		$4.6^{\diamond}$	0.131	$16.93^{+6.35}_{-2.99}$
G34.7-0.4[a]	W44,	284.00	1.37	0.29	Normal	**2.66 ± 0.71**	0.49	0	0	B		$2.1^{\star}/2.8^{\circ}/3.0^{\bullet}$	0.713	$17.71^{+6.64}_{-3.12}$

Wang+(2020)

Distance and extinction of 34 SNRs measured by VVV data

Wang+(2020)

Table 2. Distance and extinction of 34 SNRs measured by VVV data.

Name [(a)]	Other name	RA (deg)	Dec (deg)	Radius (deg)	RC ridge [(b)]	$(d_{ext})_P$ [(c)] (kpc)	$(\Delta A_{K_S})_P$ (mag kpc^{-1})	$(d_{ext})_S$ [(d)] (kpc)	$(\Delta A_{K_S})_S$ (mag kpc^{-1})	Reliability	d_{rad} [(e)] (kpc)	d_{other} [(f)] (kpc)	$(A_{K_S})_{SNR}$ (mag)	Dust mass ($M_\odot$)
G3.8+0.3		268.23	−25.47	0.15	Normal	**4.14 ± 0.29**	0.32	0	0	A	6.4		0.399	$8.25^{+3.10}_{-1.46}$
G5.4-1.2[a]	Milne 56	270.54	−24.90	0.29	Normal	**3.89 ± 0.37**	0.14	0	0	A		>4.3	0.235	$16.22^{+6.08}_{-2.86}$
G6.1+1.2		268.73	−23.08	0.25	Normal	**3.67 ± 0.36**	0.12	0	0	A	6.7		0.197	$7.71^{+2.89}_{-1.36}$
G6.4-0.1[a]	W28	270.13	−23.43	0.40	KDE	**3.55 ± 0.34**	0.56	0	0	A		1.9	0.772	$83.30^{+31.24}_{-14.70}$
G6.5-0.4		270.55	−23.57	0.15	Normal	**3.72 ± 0.21**	0.70	0	0	A	4.1		0.578	$9.60^{+3.60}_{-1.69}$
G8.7-0.1[a]	W30	271.38	−21.43	0.38	KDE	**4.15 ± 0.19**	0.62	0	0	B	1.9	4.5^	0.573	$74.37^{+27.89}_{-13.12}$
G8.9+0.4		270.99	−21.05	0.20	KDE	**3.51 ± 0.41**	0.21	0	0	A	4.3		0.338	$8.91^{+3.34}_{-1.57}$
G296.1-0.5		177.79	−62.57	0.31	KDE	**3.80 ± 0.50**	0.09	0	0	C		3.0 ± 1.0*	0.195	$9.68^{+3.63}_{-1.71}$
G301.4-1.0		189.48	−63.82	0.31	Normal	**2.74 ± 0.55**	0.12	0	0	A	5.2		0.254	$6.04^{+2.27}_{-1.07}$
G308.8-0.1		205.63	−62.38	0.25	Normal	**3.92 ± 0.60**	0.28	0	0	A		$6.9^{+8.1}_{-2.9}$*	0.885	$30.30^{+11.36}_{-5.35}$
G309.8+0.0		207.63	−62.08	0.21	Normal	**3.12 ± 0.22**	0.38	5.61 ± 0.42	0.3	A	4		0.497	$8.52^{+3.20}_{-1.50}$
G312.4-0.4[a]		213.25	−61.73	0.32	Normal	**4.41 ± 0.50**	0.25	0	0	C	2.4	>6/>14/$6.0^{+8.0}_{0.0}$*	0.600	$62.50^{+23.44}_{-11.03}$
G315.4-0.3		218.98	−60.60	0.20	Normal	**3.31 ± 0.28**	0.26	5.94 ± 0.36	0.25	C			0.351	$4.48^{+1.68}_{-0.79}$
G315.9+0.0		219.60	−60.18	0.21	KDE	**3.71 ± 0.18**	0.61	0	0	A	8.2		0.517	$9.25^{+3.47}_{-1.63}$
G316.3+0.0	MSH 14-57	220.38	−60.00	0.24	Normal	**3.84 ± 0.30**	0.55	0	0	C	4.1	>7.2/7.2 ± 0.6*	0.810	$18.04^{+6.76}_{-3.18}$
G318.2+0.1		223.71	−59.07	0.33	KDE	**3.27 ± 0.44**	0.45	0	0	A			0.870	$48.25^{+18.10}_{-8.52}$
G318.9+0.4		224.63	−58.48	0.25	Normal	**3.50 ± 0.32**	0.28	0	0	A			0.401	$7.68^{+2.88}_{-1.36}$
G320.4-1.2	MSH 15-52, RCW 89	228.63	−59.13	0.29	Normal	**3.00 ± 0.45**	0.08	5.85 ± 0.22	0.05	C		5.2	0.185	$7.58^{+2.84}_{-1.34}$

Extinction law

- Supernovae: 10^{51} erg
- Strong shock destroys the ambient interstellar dust and alters the size of the dust grains (Lakićević et al. 2015)
- Whether the grains become smaller or bigger is unclear
  - Sputtering: the energetic particles (v > 150 km/s) knock atoms off the grain surface (Dwek et al. 1996), a deficit of small grains in SNRs
  - Shattering: dominant in slow shocks (v~50-80 km/s) mainly destroys big grains, a deficit of big grains (Jones et al. 1994).
  - Nozawa et al. (2007) modeled the process of dust evolution in SNRs
    - The survival of dust in SNRs depends on the density of the ambient medium
    - **Silicate dust may be more easily influenced than carbonaceous dust**

Dust model: graphite and silicate, Msil/Mgra = 2:1. $n(a) \propto a^{-\alpha}$

Band: G_{BP}, r_{P1}, G, i_{P1}, G_{RP}, J, H, Ks, W1, W2 $$A_\lambda = 1.086 \int_{a_{min}}^{a_{max}} C_{ext}(\lambda, a) \frac{dN}{da} da$$

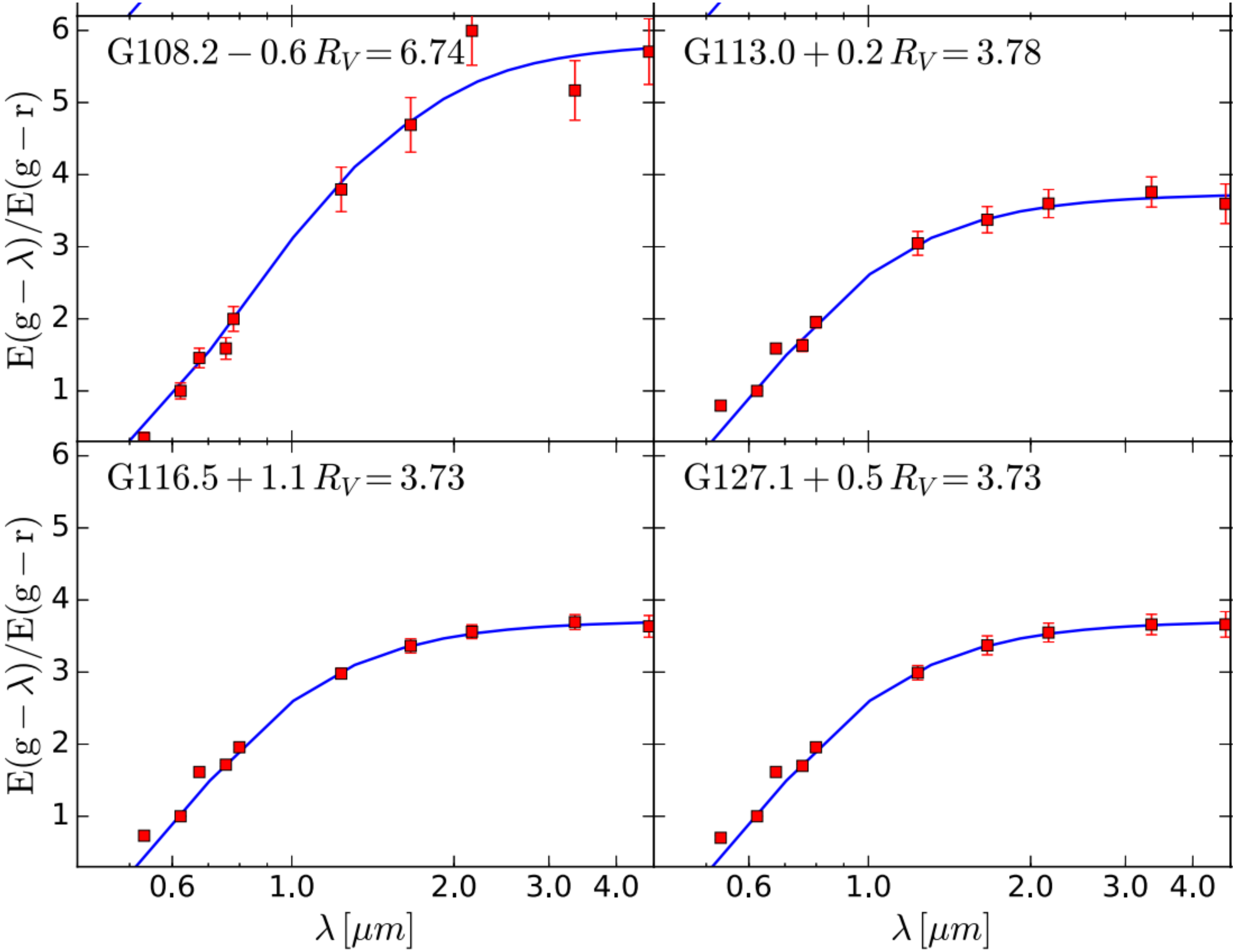

Part III: Distances to the Molecular Clouds

UV bands: GALEX/FUV and NUV
Low extinction at high latitude

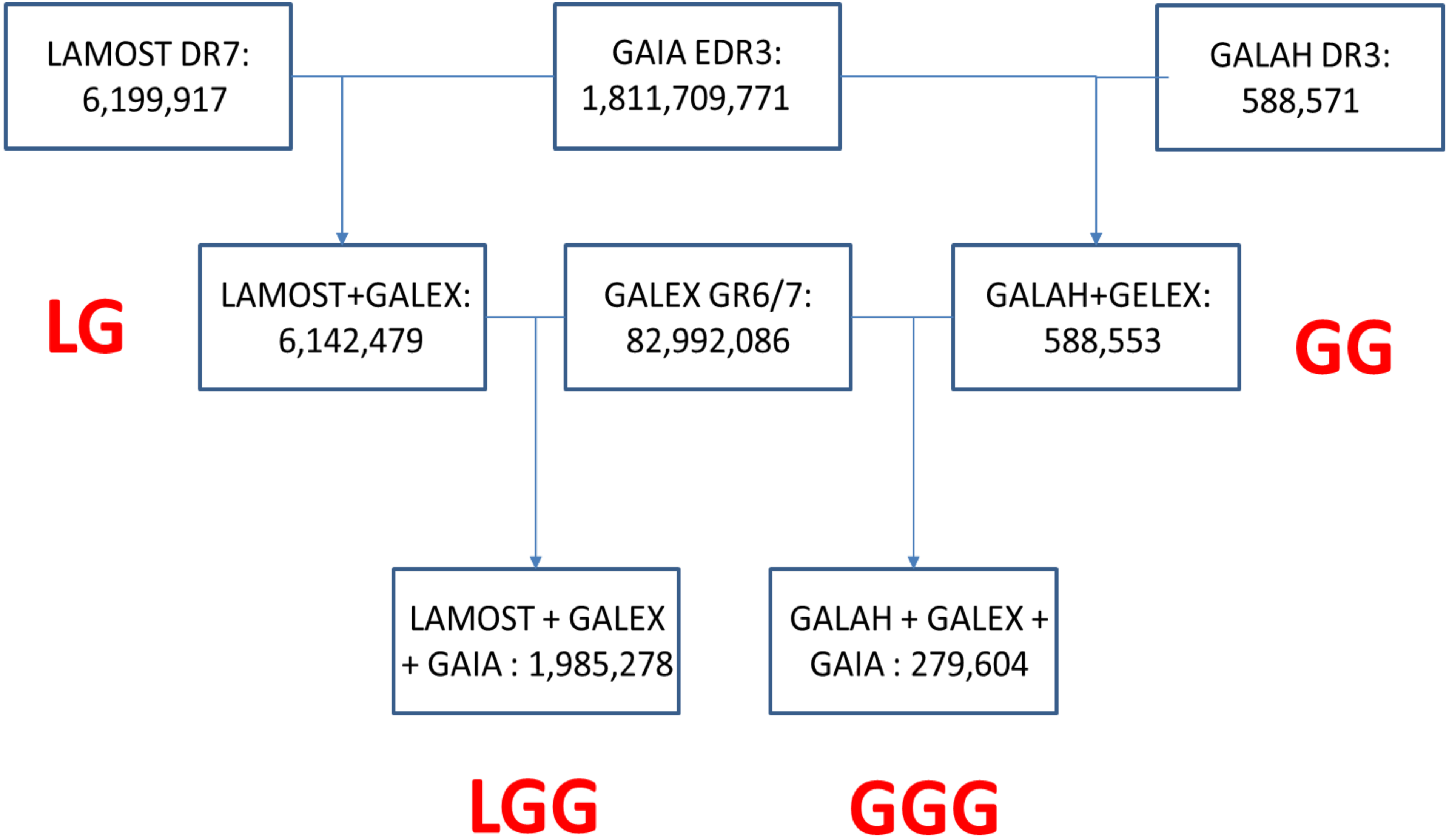

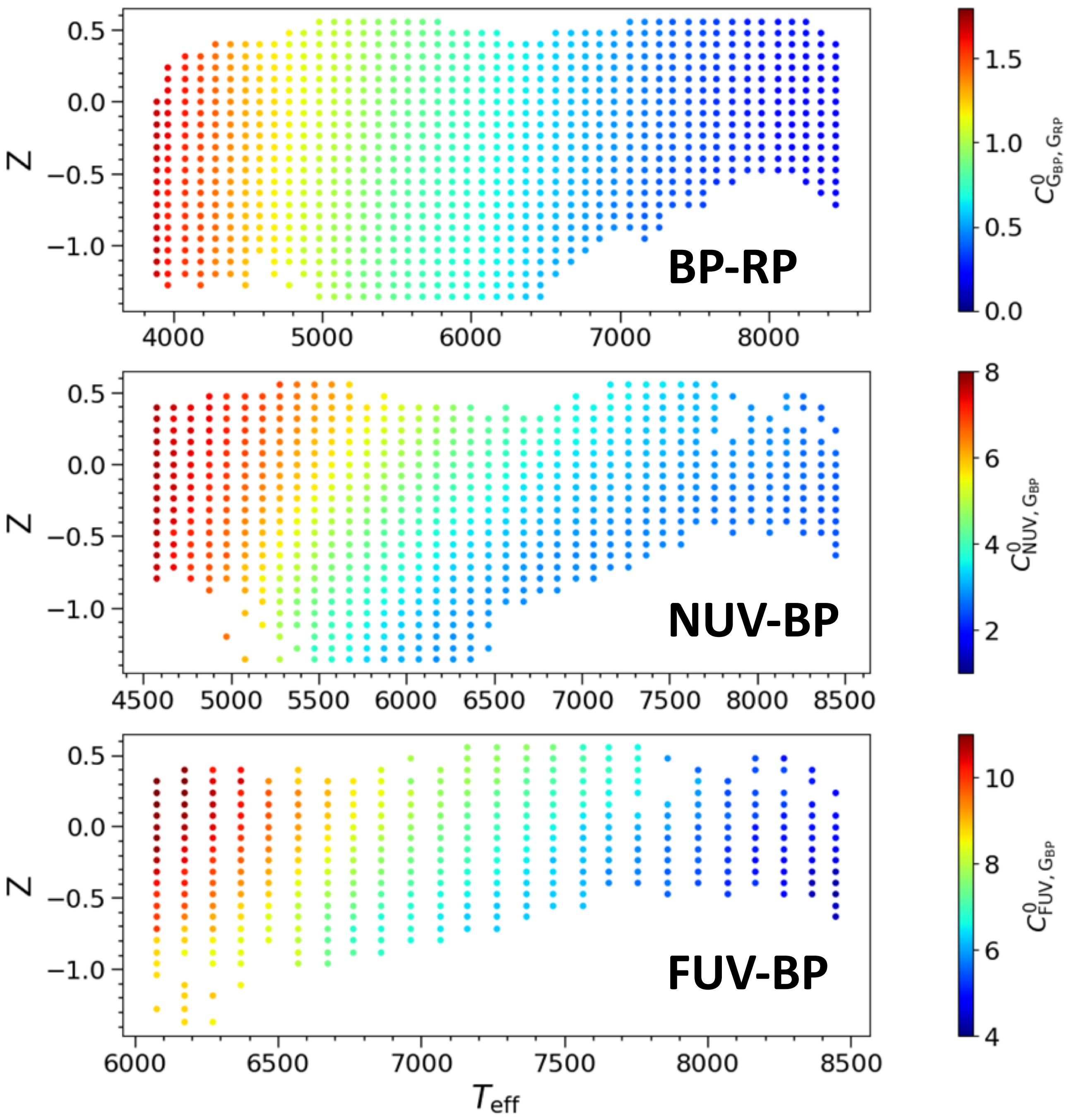

- In the UV bands, the color index is highly sensitive to metallicity
- Numerical solution to the intrinsic color indexes by the blue-edge method

Sun+2021a

$E(G_{BP}-G_{RP})$

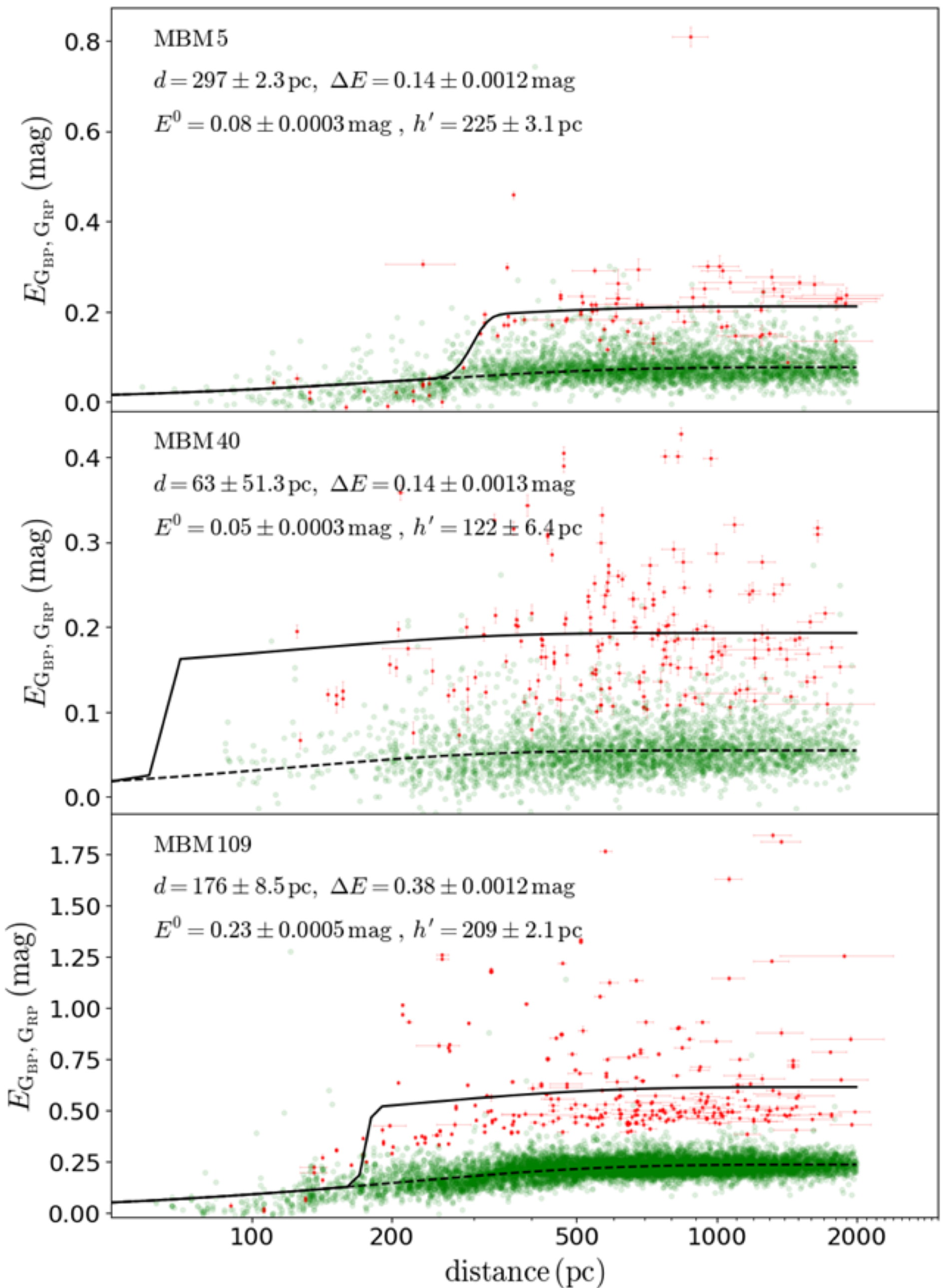

$E(NUV-G_{BP})$

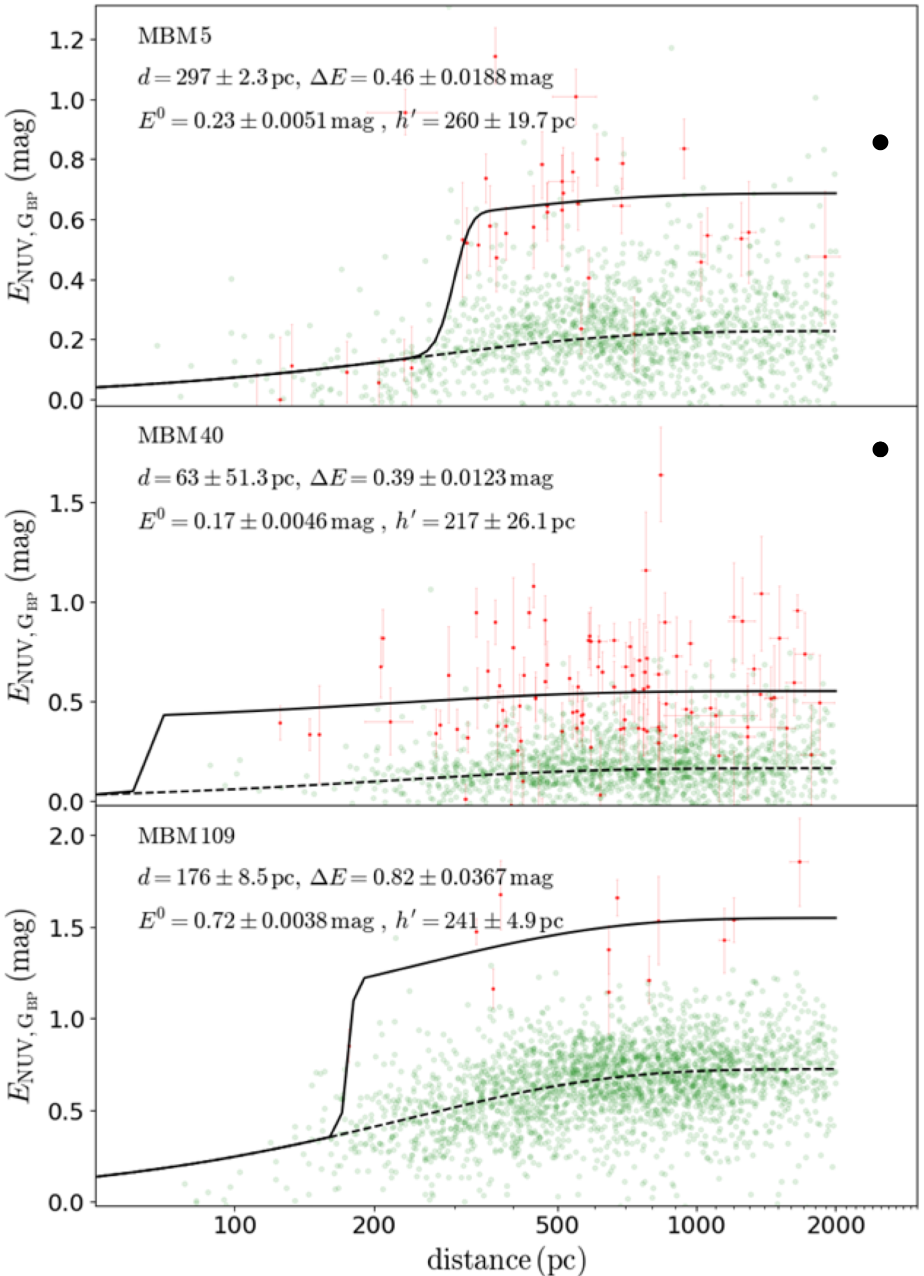

- Distances to 66 MBM molecular clouds
- Slightly larger than Schlafly+2014's, more close to Zucker+2019's
- Derived scale height of dust disk ~50-250 pc, consistent with the gaseous disk, and increasing with distance at the anti-Galactic-center direction expected from the flaring model

Sun+2021b

Structure of nearby molecular clouds (Cao+2023)

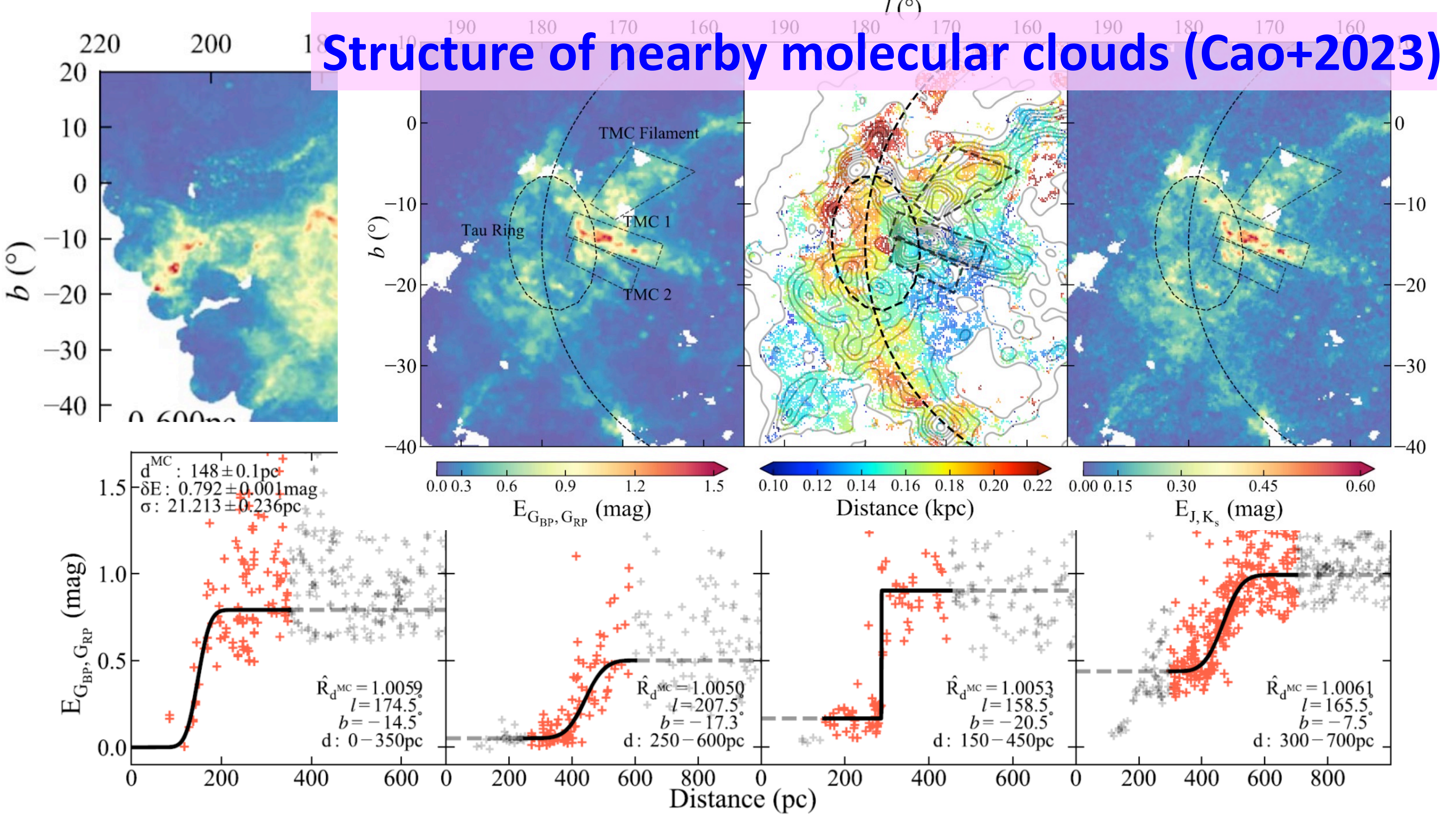

Summary

- The extinction derived from spectroscopy
  - Independent of any priors on the Galactic structure
  - Useful to trace the extinction law
  - high accuracy that can detect low-extinction
- Multiple application
  - Determination of the distances to extended objects
  - Structures of the extended objects and the Galaxy
  - Study of dust properties in various environments

Thank you